Title

Fucosylated Human Milk Oligosaccharide Foraging within the Species Bifidobacterium pseudocatenulatum Is Driven by Glycosyl Hydrolase Content and Specificity

Journal

Applied and Environmental Microbiology, 88(2)

ISSN

0099-2240

Authors

Shani, Guy
Hoeflinger, Jennifer L
Heiss, Britta E
et al.

Publication Date

2022-01-25

DOI

10.1128/aem.01707-21

Peer reviewed

AMERICAN SOCIETY FOR MICROBIOLOGY | Applied and Environmental Microbiology®

FOOD MICROBIOLOGY

Fucosylated Human Milk Oligosaccharide Foraging within the Species *Bifidobacterium pseudocatenulatum* Is Driven by Glycosyl Hydrolase Content and Specificity

Guy Shani,[a]* Jennifer L. Hoeflinger,[a§] Britta E. Heiss,[a◊] Chad F. Masarweh,[a] Jules A. Larke,[b] Nick M. Jensen,[a] Saumya Wickramasinghe,[a] Jasmine C. Davis,[c] Elisha Goonatilleke,[c] Amr El-Hawiet,[d,e] Linh Nguyen,[e] John S. Klassen,[e] Carolyn M. Slupsky,[b,f] Carlito B. Lebrilla,[c,f] David A. Mills[a,f,g]

[a]Department of Food Science and Technology, University of California Davis, Davis, California, USA
[b]Department of Nutrition, University of California Davis, Davis, California, USA
[c]Department of Chemistry, University of California Davis, Davis, California, USA
[d]Department of Pharmacognosy, Faculty of Pharmacy, Alexandria University, Alexandria, Egypt
[e]Alberta Glycomics Centre and Department of Chemistry, University of Alberta, Edmonton, Alberta, Canada
[f]Foods for Health Institute, University of California Davis, Davis, California, USA
[g]Department of Viticulture and Enology, University of California Davis, Davis, California, USA

ABSTRACT Human milk enriches members of the genus *Bifidobacterium* in the infant gut. One species, *Bifidobacterium pseudocatenulatum*, is found in the gastrointestinal tracts of adults and breastfed infants. In this study, *B. pseudocatenulatum* strains were isolated and characterized to identify genetic adaptations to the breastfed infant gut. During growth on pooled human milk oligosaccharides (HMOs), we observed two distinct groups of *B. pseudocatenulatum*, isolates that readily consumed HMOs and those that did not, a difference driven by variable catabolism of fucosylated HMOs. A conserved gene cluster for fucosylated HMO utilization was identified in several sequenced *B. pseudocatenulatum* strains. One isolate, *B. pseudocatenulatum* MP80, which uniquely possessed GH95 and GH29 α-fucosidases, consumed the majority of fucosylated HMOs tested. Furthermore, *B. pseudocatenulatum* SC585, which possesses only a single GH95 α-fucosidase, lacked the ability to consume the complete repertoire of linkages within the fucosylated HMO pool. Analysis of the purified GH29 and GH95 fucosidase activities directly on HMOs revealed complementing enzyme specificities with the GH95 enzyme preferring 1-2 fucosyl linkages and the GH29 enzyme favoring 1-3 and 1-4 linkages. The HMO-binding specificities of the family 1 solute-binding protein component linked to the fucosylated HMO gene cluster in both SC585 and MP80 are similar, suggesting differential transport of fucosylated HMO is not a driving factor in each strain's distinct HMO consumption pattern. Taken together, these data indicate the presence or absence of specific α-fucosidases directs the strain-specific fucosylated HMO utilization pattern among bifidobacteria and likely influences competitive behavior for HMO foraging *in situ*.

IMPORTANCE Often isolated from the human gut, microbes from the bacterial family *Bifidobacteriaceae* commonly possess genes enabling carbohydrate utilization. Isolates from breastfed infants often grow on and possess genes for the catabolism of human milk oligosaccharides (HMOs), glycans found in human breast milk. However, catabolism of structurally diverse HMOs differs between bifidobacterial strains. This study identifies key gene differences between *Bifidobacterium pseudocatenulatum* isolates that may impact whether a microbe successfully colonizes an infant gut. In this case, the presence of complementary α-fucosidases may provide an advantage to microbes seeking residence in the infant gut. Such knowledge furthers our understanding of how diet drives bacterial colonization of the infant gut.

Editor Edward G. Dudley, The Pennsylvania State University

Address correspondence to David A. Mills, damills@ucdavis.edu.

*Present address: Guy Shani, Mission College, Santa Clara, California, USA.

§Present address: Jennifer L. Hoeflinger, Mascoma, LLC, Lebanon, New Hampshire, USA.

◊Present address: Britta E. Heiss, Evolve Biosystems Inc., Davis, California, USA.

Received 25 August 2021
Accepted 31 October 2021
Accepted manuscript posted online 10 November 2021
Published 25 January 2022

KEYWORDS fucosylated HMO, *Bifidobacterium pseudocatenulatum*, α-fucosidase, substrate-binding protein, strain specificity, *Bifidobacterium*, fucosidases, glycan metabolism, milk oligosaccharides

In humans, colonization of the gut microbiome in early life is strongly influenced by various elements in human milk. Human milk is composed of lactose, fats, proteins, and numerous bioactive molecules. One key constituent known to influence the gut microbiota is human milk oligosaccharides (HMOs). These highly abundant (10 to 15 g liter^{-1}) (1) and structurally diverse bioactive molecules consist of neutral (nonfucosylated and fucosylated) and acidic sialylated oligosaccharides (2). While energetically dense, HMOs are not digested by the infant but, rather, fermented by intestinal microbes, often infant-borne bifidobacteria (3). Only one species of *Bifidobacterium*, *Bifidobacterium longum* subsp. *infantis*, has been shown to consume the full constellation of HMO structures (4–6), while isolates of other infant-borne species, including *Bifidobacterium longum* subsp. *longum* (7), *Bifidobacterium breve* (8), *Bifidobacterium kashiwanohense* (9), and *Bifidobacterium bifidum* (10), have been shown to consume portions of the HMO pool. These differential consumption phenotypes suggest that HMOs delivered to infants enrich a network of primary bifidobacterial consumers who target different components of the HMO pool. In addition, some primary consumers partially degrade HMOs externally, releasing component sugars, which are consumed by recipient strains (11, 12). Similar HMO consumption networks could be predicted from other HMO-consuming taxa like *Bacteriodes* species (13), *Akkermansia* species (14), and *Roseburia* species (15), among other taxa that degrade HMOs externally. These HMO consumption networks, along with the conditioning of the environment from production of organic acids (16) and lowering of pH (17), generated by fermentation of HMOs, likely limit entry into the infant colonic ecosystem.

The genome of *B. longum* subsp. *infantis* ATCC 15697 contains transporters, substrate-binding proteins (SBP), and glycosyl hydrolases (GH) organized in a 43-kb cluster specialized for HMO utilization (18). While other *Bifidobacterium* species exhibit growth on HMOs, none grow as robustly as *B. longum* subsp. *infantis*. Although the closely related *B. longum* subsp. *longum* can broadly consume type I core HMOs, relatively few strains are capable of metabolizing fucosylated HMOs, and none are known to consume sialylated HMOs (7). These growth differences have a clear genetic basis in *B. longum* subsp. *longum* SC596, which encodes two β-galactosidases and two α-fucosidases but lacks a sialidase (7). *B. breve* strains generally consume type I and II core HMOs (6, 8, 19), whereas fucosylated and sialylated HMO consumption is restricted to a few specific strains (8). The enzymes lacto-*N*-biosidase (20), α-fucosidase GH29 (21), and α-fucosidase GH95 (22) are necessary for extracellular cleavage of HMOs prior to importation and catabolism in *B. bifidum*. While *B. longum*, *B. breve*, and *B. bifidum* are well studied, they are not the only *Bifidobacterium* species detected in breastfed infant feces.

Bifidobacterium pseudocatenulatum is prevalent in the feces of breastfed infants (8, 16, 23–27), as well as adults (28–30). The bacterial composition of the infant and adult gut microbiome is distinct (31, 32) and attributable in part to differences in dietary intake. These dietary differences may select for distinct metabolic abilities in infant- and adult-derived *B. pseudocatenulatum* strains. Of six *B. pseudocatenulatum* isolates from a cohort of Japanese breastfed infants, only three showed growth on pooled HMOs, preferentially consuming fucosylated HMOs, which corresponded to the presence of an α-fucosidase GH95 (16). On the other hand, an adult-derived *B. pseudocatenulatum* strain 1E was unable to consume type II core HMOs, even though *in silico* analysis revealed that its genome encoded β-galactosidases and a β-hexosaminidase (30). Further research is needed to understand strain-specific HMO utilization in *B. pseudocatenulatum*. In this study, we explored the genetic basis of fucosylated HMO consumption in infant-derived, adult-derived, and other available *B. pseudocatenulatum* strains.

TABLE 1 *Bifidobacterium pseudocatenulatum* strains included in this study

Strain ID[a]	Origin	Reference
SC237	Infant feces	11
SC564	Infant feces	11
SC585	Infant feces	11
SC665	Infant feces	11
SC666	Infant feces	11
MP80	Infant feces	26
MP86	Infant feces	26
JCM7040	Human feces	
JCM11661	Unlisted	
GST210	Adult feces	This study
L15	Lamb feces	27
DSM 20438	Infant feces	

[a]JCM, Japan Collection of Microorganisms; DSM, German Collection of Microorganisms and Cell Cultures.

RESULTS

Isolation and phylogenetic analysis of *Bifidobacterium pseudocatenulatum*. To evaluate a diverse pool of *B. pseudocatenulatum* strains for HMO growth phenotypes, isolates were obtained from many sources (Table 1). Most *B. pseudocatenulatum* strains were obtained from earlier studies (infant derived) (8, 33), culture collections (various sources), and colleagues (lamb derived) (34). An adult-derived *B. pseudocatenulatum* GST210 was isolated from a fecal sample donated by an individual participant in a bovine milk oligosaccharide supplementation tolerance trial (35). All *B. pseudocatenulatum* isolates ($n = 62$) were characterized with multilocus sequence typing. In total, 11 unique allelic profiles were observed (data not shown) and concatenated to construct a phylogenetic tree (Fig. S1 in the supplemental material). While *B. pseudocatenulatum* DSM 20438 had an identical allelic profile to *B. pseudocatenulatum* MP86, both isolates were included in this study since they came from two very different sources. All 12 *B. pseudocatenulatum* strains are listed in Table 1.

Growth of *B. pseudocatenulatum* isolates on pooled HMOs and select purified fucosylated HMOs. Isolates of *B. pseudocatenulatum* ($n = 12$) were examined for their ability to consume pooled HMOs. All *B. pseudocatenulatum* isolates grew well on lactose (positive control, data not shown), whereas growth on pooled HMOs varied (Fig. 1A and B). The *B. pseudocatenulatum* isolates SC585, MP80, MP86, DSM 20438 (infant derived), and JCM7040 (human derived) grew to a maximum optimum density (OD) ($0.94 \leq \text{OD} \leq 1.17$) similar to the positive-control *B. longum* subsp. *infantis* ATCC 15697 (OD, 1.13) (Fig. 1A). In contrast, the *B. pseudocatenulatum* isolates SC237, SC564, SC665, SC666 (infant derived), JCM11661 (origin unknown), GST210 (adult derived), and L15 (lamb derived) grew to a maximum OD ($0.39 \leq \text{OD} \leq 0.59$), similar to the negative-control *Bifidobacterium animalis* subsp. *lactis* ATCC 27536 (OD, 0.51) (Fig. 1B). Since the purification of pooled HMOs does not remove 100% of the lactose, it is common to observe minimal growth.

Mass spectrometry was used to profile select (i.e., dominant) HMO structures from this specific pool that were consumed by each *B. pseudocatenulatum* strain via analysis of the spent media (Fig. 1C and Table S1). Isomers lacto-*N*-tetraose (LNT) and lacto-*N*-neotetraose (LNnT) were depleted (>94%) by most *B. pseudocatenulatum* isolates, but consumption was undetectable in *B. pseudocatenulatum* SC585 (infant derived), SC237, and L15 (lamb associated).

Consumption of fucosylated HMOs by *B. pseudocatenulatum* isolates varied by structure. 2′-fucosyllactose (2′-FL) and lactodifucotetraose (LDFT) were depleted almost entirely by *B. pseudocatenulatum* SC585, MP80, MP86, JCM7040, and DSM 20438 (all >97%). All *B. pseudocatenulatum* isolates exhibited some consumption of LDFT (26 to 47%). Lacto-*N*-fucopentaose type I and III (LNFP I and LNFP III, respectively) were consumed by *B. pseudocatenulatum* that consumed 2′-FL, albeit to a lesser extent (66 to 85%). Uniquely, *B. pseudocatenulatum* MP80 consumed lacto-*N*-difucohexaose type I and

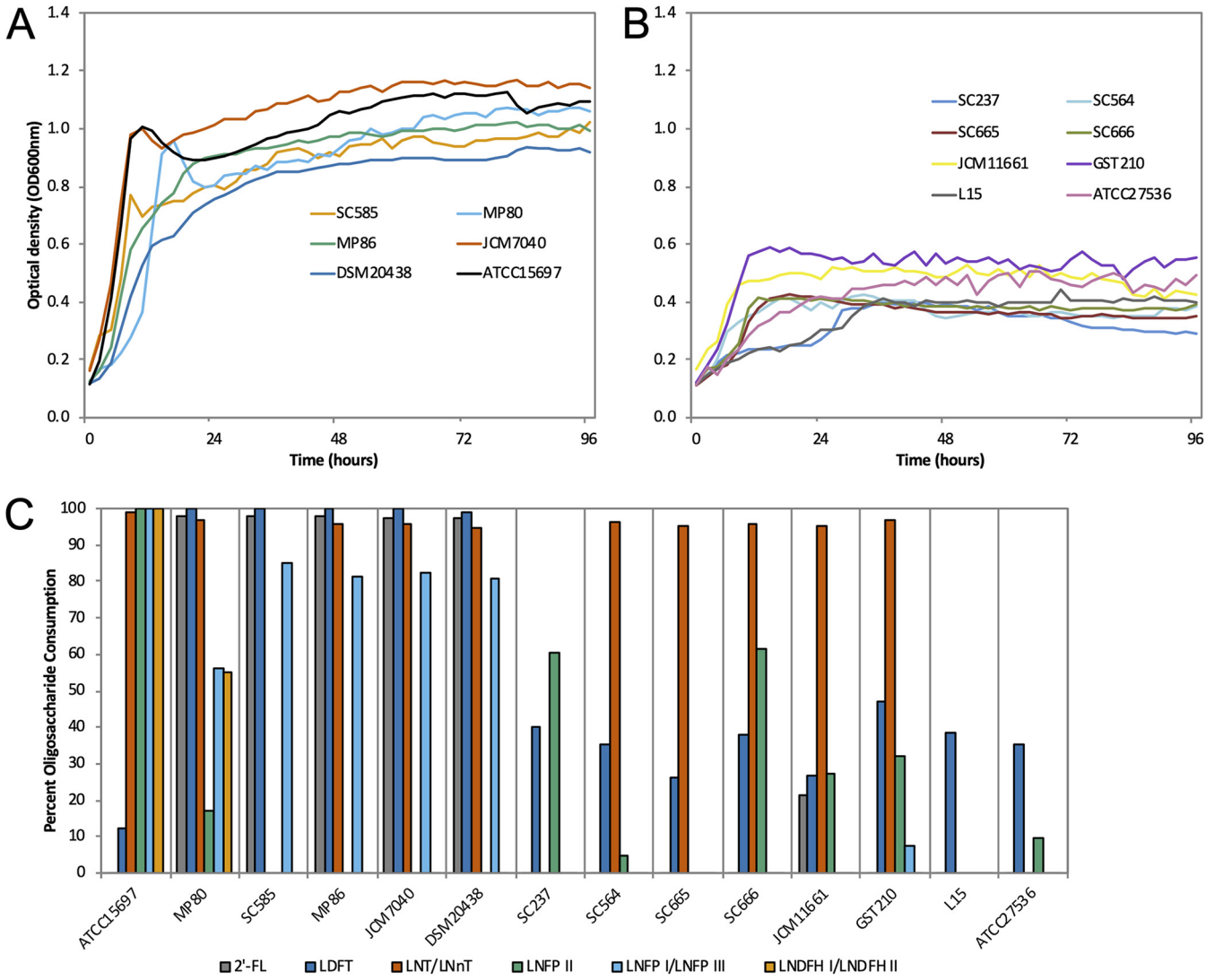

FIG 1 *B. pseudocatenulatum* growth and glycoprofiling on human milk oligosaccharides (HMOs). *B. pseudocatenulatum* isolates grown on 2% (wt/vol) pooled HMOs with strong (A) and weak (B) growth phenotypes. *B. longum* subsp. *infantis* ATCC 15697 and *B. animalis* subsp. *lactis* ATCC 27536 were included as positive and negative controls, respectively. Mean optical density at 600 nm of two independent biological replicates. (C) Glycoprofiling of the dominant HMOs from this HMO pool consumed by *B. pseudocatenulatum* isolates grown on 2% (wt/vol) HMOs. Percent consumption was calculated as the difference in HMO structure abundance at 96 h relative to 0 h. 2′-FL, 2′-fucosyllactose; LDFT, lactodifucotetraose; LNT, lacto-*N*-tetraose; LNnT, lacto-*N*-neotetraose; LNFP I, II, and III, lacto-*N*-fucopentaose type I, II, and III; LNDFH I and II, lacto-*N*-difucohexaose type I and II.

II isomers (LNDFH I and LNDFH II, 55%). *B. longum* subsp. *infantis* ATCC 15697 demonstrated an ability to consume higher-molecular-weight HMOs, whereas *B. pseudocatenulatum* isolates preferred lower-molecular-weight fucosylated HMOs (Table S1).

To explore subtle differences observed in growth on HMO pools (Fig. 1C), select *B. pseudocatenulatum* strains that grew well on HMO pools were examined for growth on purified HMO species. Strains SC585, MP80, MP86, JCM7040, and DSM 20438 grew on purified 2′-FL and 3′-fucosyllactose (3′-FL) (Fig. 2A and B). While *B. pseudocatenulatum* JCM11661 consumed 2′-FL from pooled HMOs (22%, Fig. 1C), it failed to grow robustly on purified 2′-FL as the sole carbon source (Fig. 2A). Notably, SC585 was able to grow on LNT but failed to grow on LNnT, while MP80 readily grew on both isomers (Fig. 2C). However, both MP80 and SC585 readily grew on LNFP1, which contains the LNnT type 2 core (Fig. 2D).

Growth of *B. pseudocatenulatum* MP80 on 2′-FL and lactose produced the end products acetate (44.71 mM $\pm$ 1.21 versus 44.51 mM $\pm$ 0.20; $P = 0.185$), lactate (19.06 mM $\pm$ 0.53 versus 22.79 $\pm$ 0.12; $P = 0.027$), and ethanol (0.92 mM $\pm$ 0.02, 0.35 mM $\pm$ 0.003; $P < 0.01$).

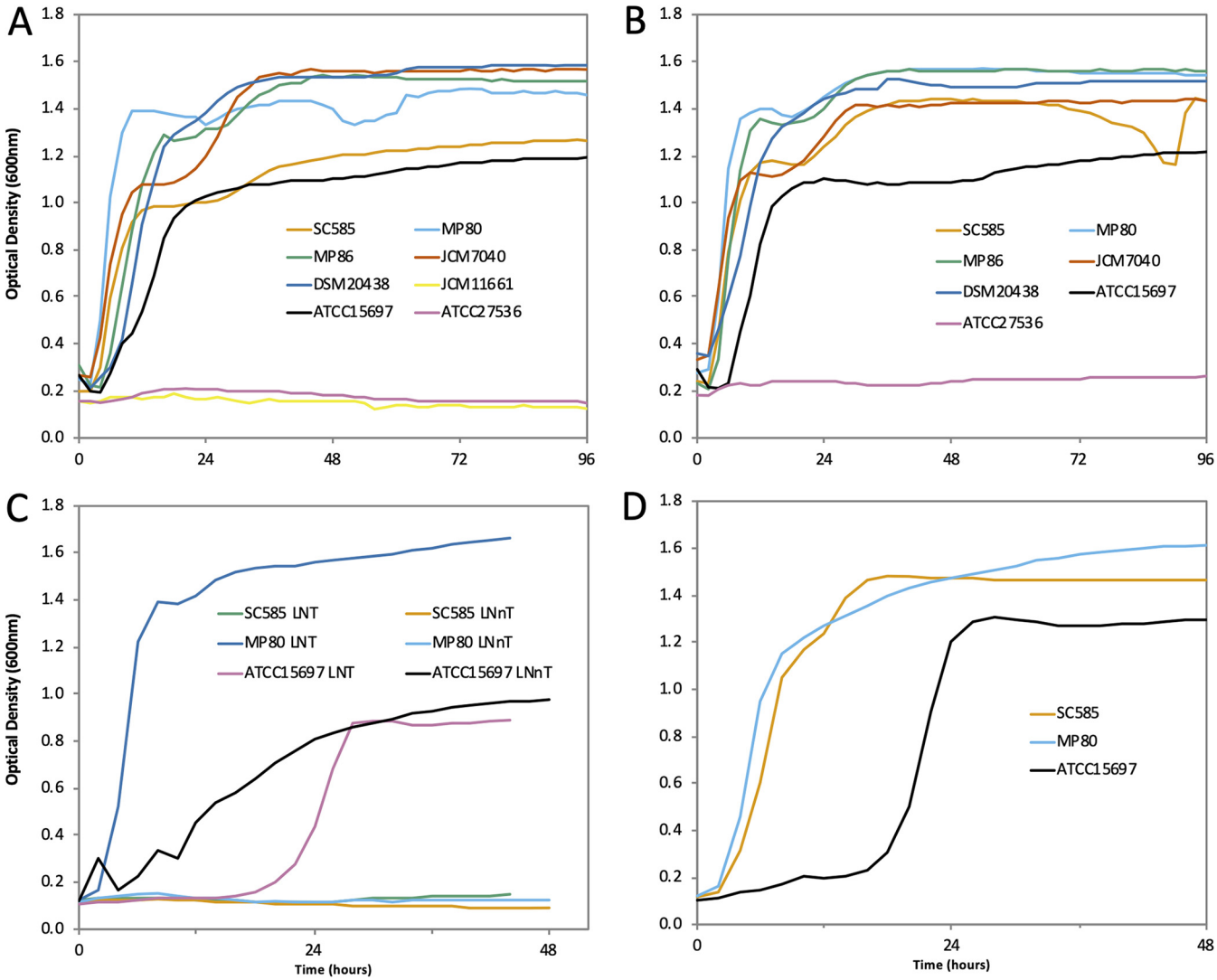

FIG 2 Subset of *B. pseudocatenulatum* isolates grown on 2% (wt/vol) 2′-fucosyllactose (A), 3′-fucosyllactose (B), lacto-*N*-tetraose and lacto-*N*-neotetraose (C), and lacto-*N*-fucopentaose I (D). *B. longum* subsp. *infantis* ATCC 15697 and *B. animalis* subsp. *lactis* ATCC 27536 were included as positive and negative controls. Mean optical density at 600 nm of two independent biological replicates.

B. pseudocatenulatum MP80 produced significantly larger amounts of formate (6.20 mM ± 0.23 versus 0.74 mM ± 0.002; $P < 0.01$), pyruvate (2.82 mM ± 0.11 versus 0.12 mM ± 0.002; $P < 0.01$), and 1,2-propanediol (2.82 mM ± 0.18 versus 0.00 mM ± 0.00; $P < 0.01$) following growth on 2′-FL than growth on lactose (Table 2). The metabolites observed provide functional validation of the MP80 fucose catabolism via the propanediol pathway observed in other fucosylated HMO (F-HMO)-consuming bifidobacterial strains (9).

Characterization of a fucosylated HMO utilization gene cluster. To identify genes required for fucosylated HMO consumption, we sequenced the genomes of

TABLE 2 Millimolar concentrations of metabolites detected in the cell-free supernatant of *B. pseudocatenulatum* MP80 grown on 1% 2′-FL versus 1% lactose[a]

	Concn (mM) of:						
Carbohydrate	Acetate	Lactate	Ethanol	Formate	Pyruvate	1,2-Propanediol	Fucose
2′-FL	44.71 ± 1.21	19.06 ± 0.53	0.92 ± 0.02	6.20 ± 0.23	2.82 ± 0.11	4.28 ± 0.18	0.65 ± 0.01
Lactose	47.51 ± 0.20	22.79 ± 0.12	0.35 ± 0.00	0.74 ± 0.00	0.12 ± 0.00	ND	ND
P value	0.185	0.027	<0.01	<0.01	<0.01	NA	NA

[a]Data are presented as mean ± SE. 2′-FL, 2′-fucosyllactose; ND, not detected; NA, not available.

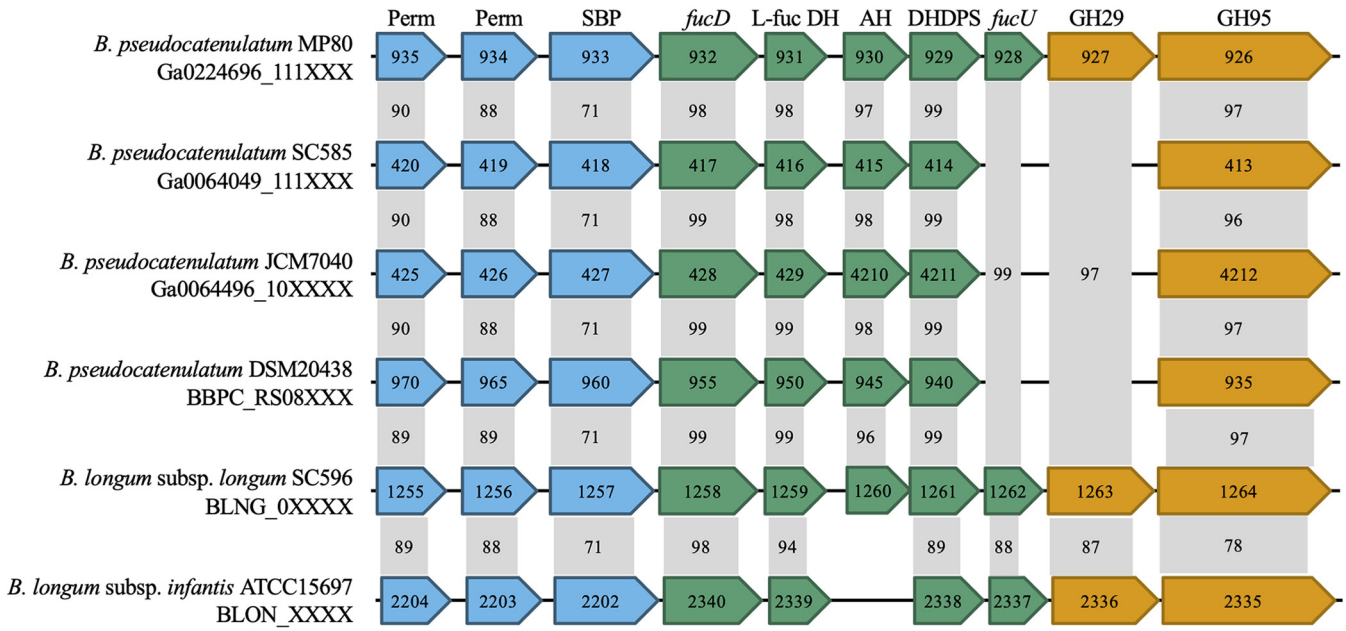

FIG 3 Schematic representation of the fucosylated HMO utilization cluster in *B. pseudocatenulatum* strains MP80, SC585, JCM7040, and DSM 20438 (GenBank accession number AP012330) and homologous genes in *B. longum* subsp. *infantis* ATCC 15697 (GenBank accession number CP001095). Partial gene locus tags are reported inside the arrows, and gene annotations are at the top. Genes are grouped by primary function as follows: oligosaccharide transport, blue; carbohydrate feeder pathways, green; and glycosyl hydrolases, orange. Numbers in gray boxes represent percent identity of amino acid sequences compared to *B. pseudocatenulatum* MP80 (BLASTp from NCBI). Perm, ABC permease; SBP, substrate-binding protein; *fucD*, L-fuconate dehydratase; L-fuc DH, L-fucose dehydrogenase; AH, amido hydrolase; DHDPS, dihydropicolinate synthase; *fucU*, L-fucose mutarotase; GH29, α-fucosidase; GH95, α-fucosidase.

B. pseudocatenulatum SC585, MP80, JCM7040, JCM11661, L15, and GST210 (refer to Table S2 for a summary of the sequencing metrics). *B. pseudocatenulatum* L15 and GST210 were included as representatives that could not consume 2′-FL. These newly sequenced *B. pseudocatenulatum* strains have comparable genome sizes and characteristics to *B. pseudocatenulatum* DSM 20438.

A cluster of genes, predicted to be associated with the consumption of F-HMOs, was readily observed in *B. pseudocatenulatum* SC585, MP80, JCM7040, and DSM 20438 (Fig. 3). Annotated genes in this cluster include two ATP-binding cassette (ABC) transporter permease components, a family 1 (oligosaccharide-binding) ABC transporter substrate-binding protein, an L-fuconate dehydratase, an L-fucose dehydrogenase, a metal-dependent hydrolase, a 4-hydroxy-tetrahydrodipicolinate synthase, and an α-fucosidase GH95. *B. pseudocatenulatum* L15 or GST210 did not contain the putative F-HMO gene cluster, consistent with their inability to robustly consume F-HMOs (Fig. 1C). Interestingly, two additional genes, a fucose mutarotase and an α-fucosidase GH29, were observed in *B. pseudocatenulatum* MP80. These additional genes are homologous to the fucose mutarotase and α-fucosidase GH29 from *B. longum* subsp. *infantis* ATCC 15697.

A survey of all publicly available *B. pseudocatenulatum* genomes in NCBI (June 2020) revealed a subset of strains possessing homologs of the fucosidase operon found in *B. pseudocatenulatum* SC585, MP80, and JCM7040 (Fig. 4). Of this subset, strains CA-C29, CA-K29a, and CA-K29b are infant derived, while the *B. pseudocatenulatum* isolates TM10-1, AF17-20AC, and AF45-10BH were isolated from human feces of an unreported age. Unique among *B. pseudocatenulatum* isolates, *B. pseudocatenulatum* MP80 possessed two α-fucosidases (GH29 and GH95) resembling the genomes of *B. longum* subsp. *infantis* ATCC 15697 and *B. longum* subsp. *longum* SC596 (7, 36). This additional fucosidase presence in MP80 and absence in the other F-HMO-consuming *B. pseudocatenulatum* strains (SC585, JCM7040, and DSM 20438) likely contributes to the differential F-HMO catabolism capacity described above. Aside from some shared ABC transporter permeases, most *B. pseudocatenulatum* strains lack homologs of the fucosidase operon entirely (Fig. 4).

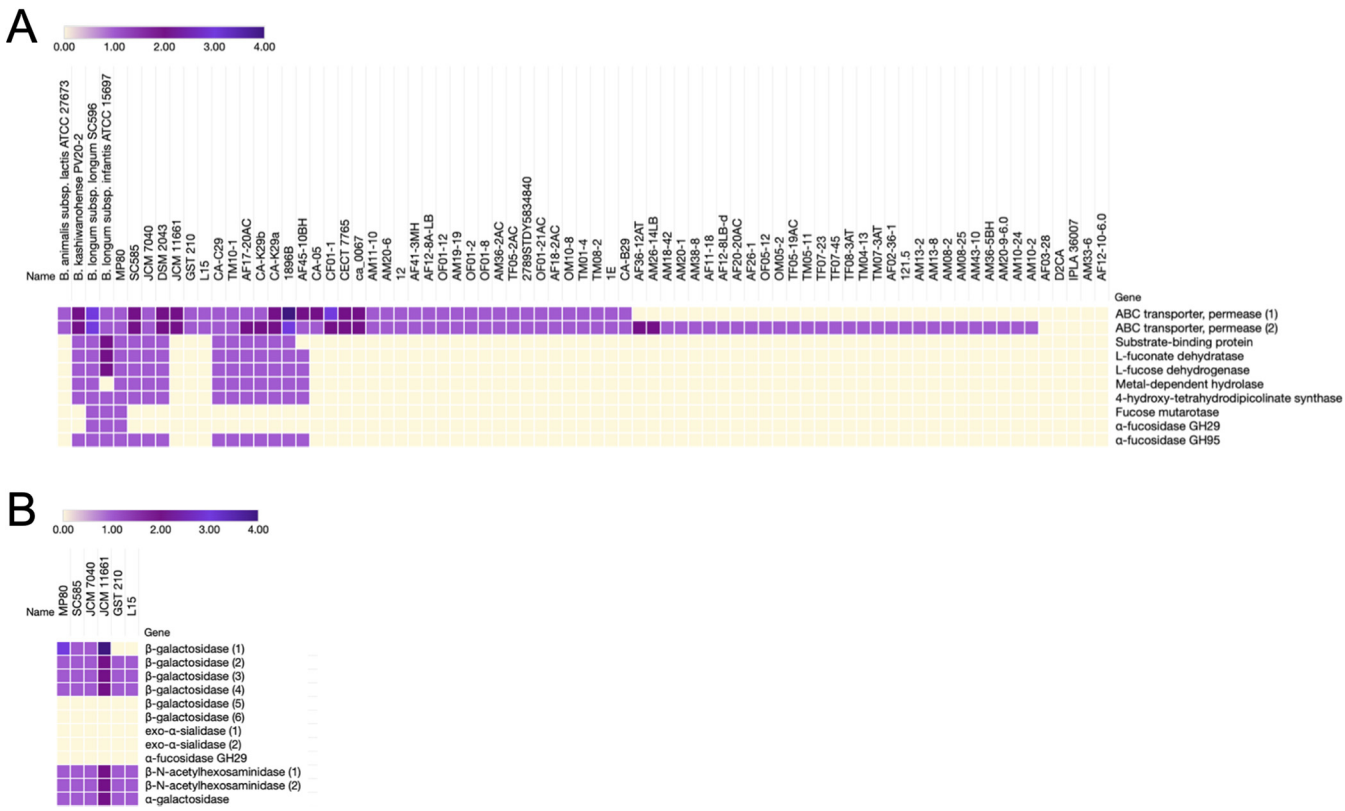

FIG 4 (A) Relative abundance of fucosidase operon homologs in publicly available *B. pseudocatenulatum* genomes. Color gradient represents the number of homologs of each gene predicted within the genomes depicted. Hierarchical clustering (Spearman rank correlation, average linkage) was performed based on the presence or absence of homologs throughout the fucosidase operon. *B. animalis* subsp. *lactis* ATCC 27673 (F-HMO$^+$), *B. kashiwanohense* PV20-2, *B. longum* subsp. *longum* SC596 (F-HMO positive [F-HMO$^+$]), and *B. longum* subsp. *infantis* ATCC 15697 (F-HMO$^+$) included for reference. *B. pseudocatenulatum* strain genome sequence accessions used are listed in Table S3 in the supplemental material. (B) Additional HMO-related glycosyl hydrolases and transporters from the six *B. pseudocatenulatum* strains glycoprofiled in this work (see Fig. 1 and 2). Homologs were predicted with PyParanoid (v0.4.1).

While the presence or absence of this main F-HMO gene cluster clearly differentiated the more robust F-HMO consumer strains (MP80, SC585, and JCM7040) from the "nonconsumers" (L15, JCM11661, and GST210), it did not explain other subtle differences in HMO consumption patterns between some strains. Notably, glycoprofiling revealed that strain SC585 did not consume LNT/LNnT (Fig. 1C). While SC585 lacked the ability to grow on LNnT and LNT, it was able to grow well on LNFP1, which contains LNnT as a core (Fig. 2D). Moreover, the shared presence of HMO-related GHs in sequenced strains MP80, JCM7040, and SC585 (Fig. 4B) does not predict the differential consumption of LNnT/LNT in these strains, demonstrating the requirement for individual strain glycoprofiling of HMO consumption preferences (from HMO pools) as well as growth on individual HMOs to truly decipher strain-level HMO-foraging behavior. At present, the mechanism underlying the lack of growth of SC585 on LNnT remains unresolved.

Transcriptomics of MP80 grown on lactose, 2′-FL, and LNFP1 revealed clear induction of the main F-HMO cluster (the cluster shown in Fig. 3) with each gene of the cluster induced from 16- to 48-fold upon growth on the two F-HMOs (Table 3). In addition, an LNB/GNB gene cluster common to many bifidobacteria, including those that do not consume F-HMOs (37) as strongly, was upregulated during growth on LNFP1 but not on 2′-FL, likely due to the fact that LNFP1 contains *N*-acetylglucosamine. This complements a previous observation of the lack of induction of the LNB/GNB cluster during growth on 2′-FL in a *B. longum* strain that harbors a similar F-HMO cluster (7). In a separate experiment using reverse transcription-quantitative PCR (qRT-PCR), strain SC585, which possessed a similar gene cluster for fucose consumption to MP80 but lacks the GH29 fucosidase, showed

TABLE 3 Expression fold changes of fucosylated HMO utilization cluster, LNB/GNB cluster, and other HMO-utilizing genes in *B. pseudocatenulatum* MP80 strain during growth in 2′-FL and LNFP1[a]

		Fold change during growth on substrates	
Gene ID	**Annotated function**	**2′-FL**	**LNFPI**
FHMO utilization cluster			
2765237614	1,2-α-L-fucosidases (GH95)	**21.71**	**16.28**
2765237615	α-1,3/1,4-L-fucosidase (GH29)	**22.24**	**16.07**
2765237616	L-fucose mutarotase	**20.35**	**15.08**
2765237617	4-Hydroxy-tetrahydrodipicolinate synthase	**26.74**	**21.77**
2765237618	Amido hydrolase	**42.09**	**48.53**
2765237619	L-fucose dehydrogenase	**40.28**	**51.69**
2765237620	L-fuconate dehydratase	**40.34**	**45.18**
2765237621	Solute-binding protein	**30.82**	**38.22**
2765237622	ABC permease	**28.41**	**38.05**
2765237623	ABC permease	**29.60**	**41.63**
2765237623	Transcriptional regulator	**2.58**	**2.61**
LNB/GNB cluster			
2765237505	*N*-acetylglucosamine-6-phosphate deacetylase	1.03	**66.36**
2765237506	Glucosamine-6-phosphate deaminase	0.60	**48.50**
2765237507	β-*N*-acetylhexosaminidase	0.60	**21.57**
2765237508	Predicted NBD/HSP70 family sugar kinase	0.51	**31.28**
2765237509	ABC permease	0.60	**12.39**
2765237510	ABC permease	0.48	**7.91**
2765237511	Type 1 HMO solute-binding protein	0.61	**2.17**
Other important HMO-utilizing genes			
2765236220	β-Galactosidase	0.97	**12.04**
2765237192	β-Galactosidase	1.92	**6.34**
2765237343	β-Galactosidase	**2.02**	1.11
2765237514	β-Galactosidase	**0.67**	0.38
2765237579	β-Galactosidase	1.36	**1.75**
2765237612	β-Galactosidase	1.92	**2.28**
2765236421	β-*N*-acetylhexosaminidase	**1.97**	0.84

[a]Level of expression is shown as fold change compared to the lactose control. Fold change values in bold have significant FDR *P* values ($P \leq 0.05$).

a similar induction of the GH95 fucosidase (Ga0064049_111413) and SBP (Ga0064049_111418) during growth on 2′-FL (Fig. S2), suggesting a common regulation across strains harboring this F-HMO gene cluster.

***B. pseudocatenulatum* MP80's α-fucosidase substrate digestion specificity.** In this work, most *B. pseudocatenulatum* strains that grow on F-HMOs only contained a single GH95 class of α-fucosidases. However, as shown in Fig. 3 and 4, MP80 contained both GH95 and GH29 type α-fucosidases, similar to those previously characterized in *B. longum* subsp. *infantis* (36) and *B. longum* subsp. *longum* SC596 (7). To understand the specificity of the MP80 α-fucosidases (GH29, Ga0224696_111927, and GH95, Ga0224696_111926), both were cloned, the enzymes purified, and their activity assessed against an HMO pool as described previously (7). While both α-fucosidases (GH29 and GH95) digested 2′-FL, the GH95 α-fucosidase showed higher activity (100%) than the GH29 α-fucosidase (42.8%) (Table 4). Overall, the GH95 α-fucosidase was more active than the GH29 α-fucosidase on 2-linked terminal fucose moieties (Table 4). Conversely, the GH29 α-fucosidase was more active than the GH95 α-fucosidase on 3- and 4-linked terminal fucose moieties (Table 4). In general, the addition of the GH29 enzyme (Ga0224696_111927) promoted cleavage of a range of HMO moieties poorly cleaved by the GH95 enzyme (Ga0224696_111926) (bolded structures in Table 4), suggesting the addition of the second α-fucosidase expanded the pool of fucosylated HMOs catabolized by MP80 by comparison to strains like SC585, which only contain a single GH95 type α-fucosidase.

TABLE 4 Percent digestion of fucosylated HMOs by α-fucosidases (GH29 and GH95) from *B. pseudocatenulatum* MP80

MW	Common name	% Digestion of: GH29	GH95	Fucose linkage(s)
490.19	2′-fucosyllactose	42.8	100	α(1-2)
855.33	**Lacto-*N*-fucopentaose II**	**100**	**18.9**	**α(1-4)**
	Lacto-*N*-fucopentaose I/III	42.3	96.5	α(1-2), α(1-3)
1220.46	**Monofucosyl-paralacto-*N*-hexaose IV**	**90.9**	**30.3**	**α(1-3)**
	4120a[a]	100	−86.5	α(1-4)
	Monofucosyllacto-*N*-hexaose III	**100**	**6.87**	**α(1-3)**
	Monofucosyllacto-*N*-hexaose I	25.4	100	α(1-2)
	Fucosyl-paralacto-*N*-hexaose III	**100**	**44.4**	**α(1-3)**
	Fucosyl-paralacto-*N*-hexaose I	4.44	100	α(1-2)
1366.51	**Difucosyl-paralacto-*N*-hexose II**	**100**	**49.4**	**α(1-3), α(1-4)**
	Difucosyllacto-*N*-hexose B	**100**	**8.80**	**α(1-3), α(1-4)**
	Difucosyllacto-*N*-hexose A	97.5	100	α(1-2), α(1-3)
	Difucosyllacto-*N*-hexose C	54.6	44.9	α(1-2), α(1, 4)
1512.57	Trifucosyllacto-*N*-hexose	100	92.5	α(1-2), α(1-3), α(1-4)
	4320a	100	100	α(1, 2), α(1-3), α(1-4)
1585.58	5130a	71.9	66.0	α(1-3)
	5130b	**100**	**−22.6**	**α(1-4)**
	Fucosyllacto-*N*-octaose	44.7	12.1	α(1-3)
	5130c	38.3	100	α(1-2)
1731.64	Difucosyllacto-*N*-neooctaose II	64.8	100	α(1-3)
	5230a	100	100	α(1-2), α(1-3)
	Difucosyllacto-*N*-neooctaose I/Difucosyllacto-*N*-octaose II	83.5	89.1	α(1-3), α(1-4)
	5230b	9.04	100	α(1-2), α(1-3)

[a]HMOs with numerical values refer to the number of hexose (first digit), fucose (second digit), GlcNac (third digit), and *N*-acetylneuraminic acid (fourth digit). MW, molecular weight; Gal, galactose; GlcNAc, *N*-acetylglucosamine. Boldface indicates those oligosaccharides preferentially cleaved by GH29.

***B. pseudocatenulatum* MP80 and SC585 fucosidase operon SBP's substrate-binding specificity.** As shown above, strains MP80 and SC585 were able to consume fucosylated HMOs; however, differences were noted, particularly consumption of higher-molecular-weight HMOs by MP80. Given that we did not witness differences in SBP and GH95 expression between MP80 and SC585, we postulated that ATP transporter specificity differences between the strains might also drive the HMO consumption differences in addition to the added GH29 fucosidase in MP80. Notably, the SBPs from each strain (Ga00224696_111993 versus Ga0064049_111418) were only 71% identical by comparison to the higher identity among the remaining genes in this operon between the two strains (Fig. 3), which is clearly different than the near-identical homology among the remaining genes in the cluster. The SBPs from *B. pseudocatenulatum* MP80 and SC585 were cloned and purified, and substrate-binding affinity to a variety of HMO structures was determined using catch-and-release electrospray ionization-mass spectrometry (CaR-ESI-MS) (38, 39). 2′-FL and 3′-FL had the strongest binding affinity to SBPs from both *B. pseudocatenulatum* MP80 and SC585 (Fig. 5). Several fucosylated HMOs, including 2-, 3-, and 4-linked terminal fucose moieties, showed a moderate binding affinity to SBPs from *B. pseudocatenulatum* MP80 and SC585. Specifically, *B. pseudocatenulatum* SC585's SBP moderately bound fucosylated HMOs with smaller ($\leq$4 monomers) and unbranched backbone structures (3′-sialyl Lewis A and blood group A antigen tetraose type 5). Of note, *B. pseudocatenulatum* MP80's SBP uniquely bound to longer ($>$4 monomers) and branched backbone structures (difucosyllacto-*N*-hexaose A and difucosyl-para-lacto-*N*-hexaose II). Sialylation did not prevent binding of either strain's SBP, and binding affinity did not require fucosylation. A complete list of HMO structures evaluated is presented in Tables S4 and S5.

DISCUSSION

HMOs serve as a nutritional source for the proliferation of *Bifidobacterium* species in breastfed infants (40, 41). The relative abundance and composition of *Bifidobacterium* species are correlated with maternal secretor status (33), and fucosylated HMO-consuming *Bifidobacterium* species promote beneficial intestinal metabolite profiles and

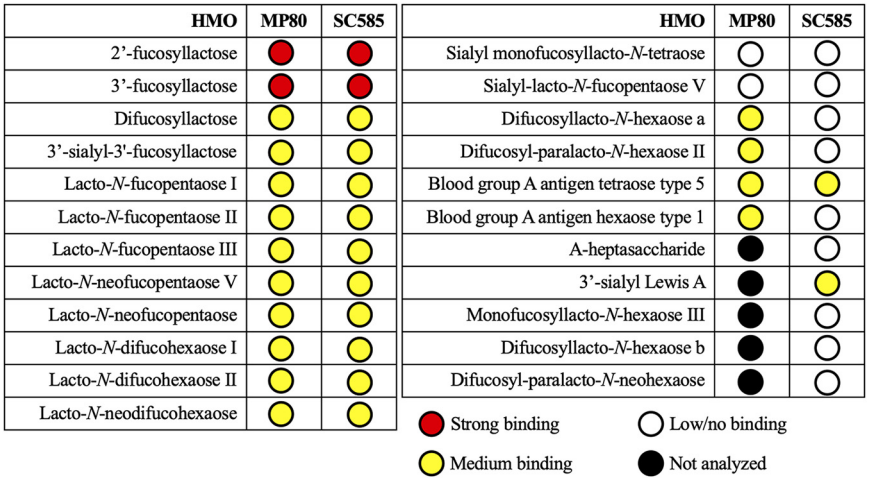

FIG 5 Binding specificity of *B. pseudocatenulatum* MP80 and SC585's substrate-binding protein to fucosylated HMO. Affinities of the HMOs were ranked according to the abundances of ligands released from the protein complexes (for details, refer to Materials and Methods).

microbiome compositions (16). *B. pseudocatenulatum* is a frequently detected member in the mammalian gut microbiota (30), including in breastfed infants (8, 16, 23–27) and adults (28–30). Therefore, it is important to examine the genomic diversity of *B. pseudocatenulatum* strains to understand its presence in several distinct ecological contexts. Unlike other species common to breastfed neonates such as *B. longum* subsp. *infantis*, *B. longum* subsp. *longum*, *B. breve*, or *B. bifidum*, *B. pseudocatenulatum* has been poorly studied despite its frequent presence in breastfed infant feces. In this study, a fucosylated HMO utilization gene cluster was identified and characterized in a subset of infant-derived *B. pseudocatenulatum* strains.

Presence of a fucosylated HMO gene cluster drives strain-dependent utilization. Growth studies revealed a subset of HMO-consuming *B. pseudocatenulatum* isolates originating from breastfed infants. Unlike these strains, other tested *B. pseudocatenulatum* isolates, including infant-, adult-, and lamb-derived specimens, poorly consumed HMOs as a sole carbon source. It was not surprising to observe poor consumption of HMOs in the adult- and lamb-derived *B. pseudocatenulatum* since HMOs are not a part of an adult or lamb's diet. However, the differential HMO consumption in infant-derived *B. pseudocatenulatum* isolates may be due to the presence or absence of HMO catabolism genes.

Bifidobacterium species possess highly specialized HMO utilization gene clusters, which promote assimilation and catabolism of neutral nonfucosylated/nonsialylated, neutral fucosylated, and acidic sialylated HMOs (42). Not all isolated *Bifidobacterium* strains from breastfed infants are capable of consuming all HMO isomers due to missing, incomplete, or dysfunctional HMO utilization gene clusters (8, 16, 27, 43–45). Whole-genome sequencing of *B. pseudocatenulatum* SC585, MP80, and JCM7040 (all infant derived) revealed an intact fucosylated HMO utilization gene cluster containing oligosaccharide transporters, a carbohydrate feeder pathway, and glycosyl hydrolase genes (Fig. 3). This gene cluster's structure and composition are homologous to the fucosylated HMO utilization gene clusters in *B. longum* subsp. *infantis* ATCC 15697 (18), *B. longum* subsp. *longum* SC596 (7), *Bifidobacterium kashiwanohense* PV20-2 (9), and other *B. pseudocatenulatum* isolates (16) (Fig. 4).

A broad analysis of publicly available *B. pseudocatenulatum* genomes illustrates a subset of *B. pseudocatenulatum* strains uniquely capable of consuming fucosylated HMOs (Fig. 4). Additionally, *B. pseudocatenulatum* MP80 is unique among *B. pseudocatenulatum* isolates given that it possesses two α-fucosidases (GH29 and GH95). This gene cluster was missing in the fucosylated HMO-nonconsuming *B. pseudocatenulatum* strains

JCM11661, L15, and GST210 included in this study. Previous studies and our analysis (Fig. 4) demonstrate that the presence or absence of genes within this gene cluster separates *B. pseudocatenulatum* strains into either consumers or nonconsumers of fucosylated HMOs (16, 27). Matsuki and colleagues (16) concluded that the fucosylated HMO utilization pathway, present in other isolated *Bifidobacterium* species as well as a subset of *B. pseudocatenulatum*, was fundamental in their cohort of Japanese infants (n = 12). Infants consuming breastmilk from secretor mothers and harboring fucosylated HMO-consuming *Bifidobacterium* species (B1 cluster) were characterized by lower fecal pH and higher concentrations of fecal acetate. They concluded that fucosylated HMO-consuming *Bifidobacterium* species, including *B. pseudocatenulatum*, produce metabolites which bestow health benefits to infants.

***B. pseudocatenulatum* MP80, a robust fucosylated HMO consumer, possesses complementary α-fucosidases (GH29 and GH95).** Previous characterization of the fucosylated HMO utilization gene cluster in *B. pseudocatenulatum* strains found that a single α-fucosidase belonging to the GH95 family was associated with consumption of 2′-FL (16, 27) and other fucosylated HMOs (16). However, the genome of *B. pseudocatenulatum* MP80 contains an additional α-fucosidase (GH29), consistent with the gene clusters in *B. longum* subsp. *infantis* ATCC 15697 (18) and several other *Bifidobacterium* species (7–9, 16, 27) but not seen previously in *B. pseudocatenulatum* (16, 27). Additionally, both α-fucosidases (GH29 and GH95) were required for robust growth on 2-, 3-, and 4-linked fucosylated HMOs in *B. breve* SC95, SC154, and SC568 (8). The α-fucosidase GH29 has been shown to preferentially cleave 3- and 4-linked terminal fucose moieties (7, 21, 36), complementing the α-fucosidase GH95's preference for 2-linked fucosylated HMOs (22, 46). Enzymatic substrate digestion specificity confirmed that *B. pseudocatenulatum* MP80's α-fucosidase GH29 preferentially cleaved 3- and 4-linked terminal fucose moieties (Table 4). However, growth on 3- and 4-linked fucosylated HMOs did not require an α-fucosidase GH29 because *B. pseudocatenulatum* strains SC585, JCM7040, and DSM 20438 (lacking the α-fucosidase GH29) grew equally well on 2′-FL and 3′-FL. These data suggest that the α-fucosidase GH95 has some cross-reactivity on 3- and 4-linked fucosylated HMOs in *B. pseudocatenulatum* strains (Table 4). The catalytic specificity of α-fucosidase GH95s differs among *Bifidobacterium* species. Katayama and colleagues (22) did not observe cleavage of 3- or 4-linked fucosylated HMOs with *B. bifidum* JCM1254's extracellular GH95 α-fucosidase. However, *B. longum* subsp. *infantis* ATCC 15697 moderately cleaved 3-linked fucosylated HMOs (46) and several *B. breve* strains consumed 3′-FL with a single α-fucosidase GH95 and no α-fucosidase GH29 (8). The amino acid sequence of the GH95 α-fucosidase in *B. pseudocatenulatum* MP80, *B. longum* subsp. *infantis* ATCC 15697 (78%), and *B. breve* JCM7019 (97%) are homologous while not being homologous to *B. bifidum* JCM 1254 (32%). While the presence of the α-fucosidase GH95 is sufficient for growth and cleavage of 3- and 4-linked fucosylated HMOs *in vitro*, substrate competition *in vivo* may still show a growth advantage to *Bifidobacterium* possessing the complementary α-fucosidase GH29.

Expanded fucosylated HMO consumption in *B. pseudocatenulatum* MP80 cannot be attributed to a more divergent substrate-binding protein. The *B. longum* subsp. *infantis* ATCC 15697 genome encodes a plethora of family 1 SBPs to facilitate transport of HMOs via ABC permeases (18, 47). The *B. longum* subsp. *infantis* ATCC 15697 SBP (Blon_2202) and ABC permeases (Blon_2203-2204) are homologous (71 to 90% identical amino acid sequences) to the *B. pseudocatenulatum* MP80 SBP (Ga0224696_111933) and ABC permeases (Ga0224696_111934-111935). The *B. longum* subsp. *infantis* ATCC 15697 SBP (Blon_2202) has been shown to bind fucosylated HMOs (47, 48). Given its proximity to fucosylated HMO catabolism genes and homology to *B. longum* subsp. *infantis* ATCC 15697's SBP (Blon_2202), it is hypothesized that the SBP from *B. pseudocatenulatum* MP80 (Ga0224696_111933) also binds fucosylated HMOs. Catch-and-release electrospray ionization-mass spectrometry showed moderate to strong binding of *B. pseudocatenulatum* MP80's SBP (Ga0224696_111933) to 2-, 3-, and 4-linked fucosylated HMOs (Fig. 5). Recently, the crystal structure and ligand-binding site of *B. longum* subsp. *infantis* ATCC 15697's SBP

(Blon_2202) was resolved for binding both 2′-FL and 3′-FL with a rotation of 50° to accommodate the different fucose moiety linkages (48). Therefore, the strong binding affinity for both 2′-FL and 3′-FL observed with *B. pseudocatenulatum* MP80's SBP (Ga0224696_111933) was not unexpected. Additionally, *B. pseudocatenulatum* MP80's SBP (Ga0224696_111933) moderately bound to several larger (DP >3) 2-, 3-, and 4-linked fucosylated HMOs. Sakanaka and colleagues (48) suggest that the binding pocket features of *B. longum* subsp. *infantis* ATCC 15697's SBP (Blon_2202) would likely accommodate larger fucosylated HMOs (DP >3) at lower affinities (48). Along with the presence of the α-fucosidase GH29, the divergent SBP (Ga0224696_111933) in *B. pseudocatenulatum* MP80 may allow access to a broader range of fucosylated HMO catabolism.

The infant-derived *B. pseudocatenulatum* SC585 strain, possessing one α-fucosidase (GH95), consumed less diverse fucosylated HMO structures (Fig. 1C) than *B. pseudocatenulatum* MP80. The homologous SBP (Ga0064049_111418) from *B. pseudocatenulatum* SC585 differed in amino acid sequence (71% similar), perhaps suggesting a slightly lower binding specificity for fucosylated HMOs. However, catch-and-release electrospray ionization-mass spectrometry assay did not show a significant difference in the binding specificity between the SBPs from *B. pseudocatenulatum* MP80 and SC585. This result was not surprising given the greater homology (91% amino acid sequence) between the SBPs from *B. pseudocatenulatum* SC585 (Ga0064049_111418) and *B. longum* subsp. *infantis* ATCC 15697 (Blon_2202) and suggests that *B. pseudocatenulatum* MP80's complementary α-fucosidases (GH29 and GH95) promote expanded fucosylated HMO consumption capability compared to other infant-derived *B. pseudocatenulatum* strains.

Conclusions. *B. pseudocatenulatum* is a widely dispersed species isolated from a number of diverse environments. This study, among others, demonstrates a genetic basis for specialized fucosylated HMO consumption in a subset of *B. pseudocatenulatum* strains isolated from breastfed infants (16, 27). In particular, the fucosylated HMO utilization gene cluster from *B. pseudocatenulatum* MP80 indicates that the presence of complementary α-fucosidases (GH29 and GH95) may provide an advantage to residence in the infant gut.

MATERIALS AND METHODS

Isolation and identification of *Bifidobacterium pseudocatenulatum* strains. To isolate adult-derived *B. pseudocatenulatum*, 100 mg feces were vortexed in 900 μl sterile 1× phosphate-buffered saline (PBS), pH 7.4, serially diluted 10-fold in PBS, and plated (50 μl) onto modified *Bifidobacterium* selective iodoacetate mupirocin (BSIM) (33). Plates were incubated at 37°C for 48 h anaerobically (5% CO_2, 5% H_2, and 90% N_2; Coy Laboratory Products). Colonies were streaked for three successive passages onto deMan, Rogosa, and Sharpe supplemented with 500 mg liter^{-1} L-cysteine-HCl (MRSC) agar and subcultured into MRSC broth and stored at −80°C in 25% (vol/vol) glycerol. Additional strains of *B. pseudocatenulatum* (Table 1) were obtained from the American Type Culture Collection (ATCC), the Japanese Collection of Microorganisms (JCM), German Collection of Microorganisms and Cell Cultures (DSM), and previous isolation studies (8, 33, 34). Identities of *B. pseudocatenulatum* strains were confirmed by matrix-assisted laser desorption ionization–time of flight biotyper mass spectrometry as previously described (33).

Multilocus sequence typing of *B. pseudocatenulatum* isolates. The intragenic regions of seven housekeeping genes (*clpC*, *fusA*, *gyrB*, *ileS*, *purF*, *rplB*, and *rpoB*) were selected based on previous work (49). Primers (Table 2) were optimized using the publicly available *B. pseudocatenulatum* DSM 20438 genome (GenBank accession number AP012330). Genomic DNA was extracted with the MasterPure Gram-positive DNA purification kit (Epicentre) and amplified on a PTC-200 Peltier thermal cycler (Bio-Rad). A 50-μl reaction mixture with 1 μl extracted DNA, 1 μl of each primer (10 μM), 1 μl dNTPs, 5 μl 10× PCR buffer, 5 μl $MgCl_2$, and 0.25 μl (1.25 U) AmpliTaq Gold DNA polymerase (Applied Biosystems) was used. Cycling parameters were 4 min at 95°C, 30 cycles of 95°C for 30 s, 63 to 67°C for 1 min, and 72°C for 1 min, followed by 7 min at 72°C. Amplification was confirmed by gel electrophoresis, and the PCR products were purified using the QiaQuick 96 PCR purification kit (Qiagen). Sequencing was performed on an ABI 3730 capillary electrophoresis genetic analyzer using BigDye Terminator chemistries at the University of California Davis DNA Sequencing Facility. The sequences were analyzed and aligned with ClustalW using BioEdit (version 7.0). Phylogenetic analysis of concatenated sequence loci was performed (version 6.0), and a minimum evolution tree was calculated (version 7.0) using the Molecular Evolutionary Genetic Analysis software.

***In vitro* consumption of human milk oligosaccharides.** *B. pseudocatenulatum* strains (Table 1) were tested for growth in the presence of pooled HMOs, purified from breast milk as described previously (50), and lactose (positive control). *B. longum* subsp. *infantis* ATCC 15697 and *B. animalis* subsp.

lactis ATCC 27536 were used as positive and negative HMO growth controls, respectively. All growths were conducted anaerobically at 37°C. *Bifidobacterium* species were cultured onto MRSC agar, incubated for 48 h, and subcultured into 500 μl MRSC broth. After 24 h of growth, 2% (vol/vol) was subcultured into 500 μl MRSC broth and incubated for 18 h. A 96-well plate containing 200 μl of modified MRS medium (mMRS) (33) supplemented with 2% (wt/vol) of pooled HMOs or lactose per well was inoculated with 4 μl of stationary-phase *Bifidobacterium* species cells. Additional inoculated wells without added carbohydrates were included as controls. All wells were covered with 50 μl of sterile mineral oil to avoid evaporation and incubated for 96 h. Optical density measurements at 600 nm (OD_{600}) using a PowerWave 340 plate reader (BioTek) were taken every 30 min, preceded by 30 s of shaking at variable speed. After growth, cell-free supernatants were collected by centrifugation at 16,000 rcf for 1 min and stored at −80°C until identification of remaining HMOs (described below). Technical triplicates of biological duplicates were performed for each bacteria and sugar combination.

A subset of the *Bifidobacterium* isolates (those able to consume 2′-FL, as well as one that could not) were tested for growth on purified 2′-FL (Glycom) and 3′-FL (Glycom) (51) using the same methods as above.

***B. pseudocatenulatum* MP80 metabolite production following growth on 2′-FL.** *B. pseudocatenulatum* MP80 was subcultured three times on MRSC broth and incubated anaerobically at 37°C for 12 h. A 5% (500 μl [vol/vol]) inoculum was added to 10 ml of mMRS supplemented with 1% (wt/vol) lactose or 2′-FL. Optical density measurements were monitored in a PowerWave 340 plate reader until late log phase (OD_{600}, ~0.8). Cells were pelleted by centrifugation at 3,220 rcf for 3 min and washed in 10 ml 1× PBS (anaerobically conditioned) and resuspended in 15 ml mMRS supplemented with 0.5% (wt/vol) lactose or 2′-FL. After 10 min of anaerobic growth, cultures were centrifuged at 3,220 rcf for 3 min at 4°C. The cellular population (CFU ml^{-1}) was calculated to determine consistency between triplicates. Cell-free supernatants were filtered through a 3-kDa-molecular-weight filter and stored at −80°C until analysis. Thawed filtrate was prepared with the addition of internal standard DSS-d6 [2,2,3,3,4,4-d6-3-(trimethylsilyl)-1-propane sulfonic acid] at a 1:10 ratio and adjusted to pH 6.8 ± 0.1 using NaOH and HCl. A 180-μl aliquot was transferred to a 3-mm Bruker nuclear magnetic resonance (NMR) tube and stored at 4°C until spectral acquisition. Spectra were acquired by 1H nuclear magnetic resonance spectroscopy as previously described (52). Fourier-transformed spectra were processed in Chenomx NMR Suite (version 8.4) followed by manual annotation of each metabolite.

***B. pseudocatenulatum* genome sequencing and comparative genomics.** To whole-genome sequence six isolates (SC585, MP80, JCM7040, JCM11661, L15, and GST210), 100 to 1,000 ng of extracted and purified genomic DNA (described previously) was sent to the Vincent J. Coates Genomics Sequencing Laboratory at University of California Berkeley. DNA was sheared using Adaptive Focused Acoustics (Covaris) followed by library preparation using the IntegenX Apollo 324 platform with 13 rounds of amplification using WaferGen library prep kits. Single-read sequencing (50 bp) was performed using the high-throughput mode on the Illumina HiSeq2000 platform. Sequencing files were concatenated using Terminal, trimmed with a maximum of 2 ambiguous base pairs, and deleted if their quality scores were below 0.5. Remaining sequences were *de novo* assembled using CLC Genomics Workbench. Subsequently, *B. pseudocatenulatum* MP80 was long-read sequenced with the single molecule real-time platform to aid in *de novo* assembly of its entire circular genome. *B. pseudocatenulatum* MP80 was streaked onto MRSC agar incubated at 37°C anaerobically; three colonies were subcultured into 2 ml of MRSC both and incubated at 37°C anaerobically overnight. Total genomic DNA (3 × 2 ml) was extracted with the DNeasy blood and tissue kit, including the pretreatment for Gram-positive bacteria (Qiagen) according to the manufacturer's instructions. Slight modifications were made, including 20 μl of 50 mg ml^{-1} lysozyme from chicken egg white and 4 U of mutanolysin, and were included in the enzymatic lysis buffer, followed by addition of proteinase K and RNase A (kit provided) and incubation for 2 min at room temperature prior to combination with the AL buffer. Total genomic DNA was eluted in 35 μl of EB and pooled (total, 105 μl). Protein contamination was measured by NanoDrop 1000, and RNA contamination and genomic DNA shearing were evaluated by gel electrophoresis. The DNA and RNA concentrations were measured using the Qubit 2.0 fluorometer and Qubit double-stranded DNA (dsDNA) BR and Qubit RNA HS sssay kits, respectively (Invitrogen). Size selection of genomic DNA (at 10,000 bp) on the BluePippin system and sequencing on the PacBio Sequel system was conducted by the DNA Technologies and Expression Analysis Cores at the University of California Davis Genome Center. The genome was assembled with the filtered_subreads.fastq file using the default parameters of Canu (version 1.6) (53). *B. pseudocatenulatum* genomes were annotated and deposited in the Integrated Microbial Genome Expert Review annotation platform (GOLD project ID Gs0113979).

Fucosidase operon gene homologs in publicly available *B. pseudocatenulatum* genomes were identified with the PyParanoid pipeline (version 0.4.1) using default parameters (54). Briefly, the FASTA amino acid files of 319 higher-quality genomes were chosen to generate alignments with DIAMOND (version 0.9.24) (55). Homologous proteins were identified with Markov cluster algorithm (MCL 14 to 137) (56) and aligned with MUSCLE (v3.8.1551) (57). Hidden Markov models of each homologous protein alignment at homology cutoff at 95% amino acid identity were created with HMMER (v3.2.1) and propagated to additional *Bifidobacterium* genomes. The resulting matrix of homolog presence or absence was filtered to *B. pseudocatenulatum* strains of interest. A heatmap of predicted homolog copy number was visualized with Morpheus (accessed on 7 July 2020) (https://software.broadinstitute.org/morpheus/).

***B. pseudocatenulatum* MP80 fucosidase operon gene expression.** Expression of the SBP (Ga0224696_111933), α-fucosidase GH29 (Ga0224696_111927), and α-fucosidase GH95 (Ga0224696_111926) from *B. pseudocatenulatum* MP80 and the SBP (Ga0064049_111418) and α-fucosidase GH95 (Ga0064049_111413) from *B. pseudocatenulatum* SC585 were quantified during growth on 2′-FL. Primers were designed with the Primer-BLAST tool at NCBI (Table 5). The *rnpA* housekeeping gene from *B. pseudocatenulatum* MP80 and SC585 (Ga0224696_112000 and Ga0064049_10607, respectively) was used for relative quantification (52). *B. pseudocatenulatum* MP80 was grown on mMRS supplemented with 2% (wt/vol) glucose or 2′-FL in a

TABLE 5 Oligonucleotide primers used in this study

Purpose	Target	PCR primer (5′–3′)	
Multilocus sequence typing[a]	*clpC*	F[b]	GAGTACCGTAAGTACATCGAG
		R	TCCTCGTCGTCAAACAGGAAT
	purF	F	GTCGGGTAGTCGCCATTG
		R	CACTCCAATTCCGACACCGA
	gyrB	F	CATGCCGGCGGCAAGTTCG
		R	CCGAGCTTGGTCTTGGTCTG
	fusA	F	ATCGGCATCATGGCTCACATCGAT
		R	CCAGCATCGGCTGAACACCCTT
	ileS	F	CGGTATCGACATAGTCGGCG
		R	ATTCCGCGTTACCAGACCATG
	rplB	F	AGGACGGCGTGCCGGCAA
		R	GCCGTGCGGGTGATCGAC
	rpoB	F	GCATCCTCGTAGTTGTASCC
		R	GGCGAACTGATCCAGAACCA
B. pseudocatenulatum MP80 gene expression	*rnpA* (Ga0224696_112000)	F	GGTATCGCGAGAAGACATCGT
		R	ACGGCATTACGCGTCACA
	α-Fucosidase GH29 (Ga0224696_111927)	F	GCTCACTTCAACCCAATGCG
		R	TTCCATAGTCAGTTCCGCCG
	α-Fucosidase GH95 (Ga0224696_111926)	F	GCTTGTCCAAAGCCACGATG
		R	TCCACTGTCTGATCCGTCCA
	Substrate-binding protein (Ga0224696_111933)	F	TTCAACCGTGCTACGAACGA
		R	GCAGAATCACCGAATGCAGG
	β-Galactosidase (Ga0224696_111500)	F	ACGTACAACCAGTTCACCCG
		R	ATGCGAGCACCTCAGTATCG
	β-Galactosidase (Ga0224696_111924)	F	ACACCAATACCACGTTCGCA
		R	CGACCTTCTGAACGACGGTT
	β-Galactosidase (Ga0224696_11522)	F	GACTACAACCCGGACCAGTG
		R	GAAATCGTACACGCCTTCGC
	β-Galactosidase (Ga0224696_111652)	F	CAGCCGGAAGAAAACCGTTG
		R	TTCCGGGTGCTTTTCGTACA
B. pseudocatenulatum SC585 gene expression	*rnpA* (Ga0064049_10607)	F	GGTATCGCGAGAAGACATCGT
		R	ACGGCATTACGCGTCACA
	α-Fucosidase GH95 (Ga0064049_111413)	F	TCCGTGCAAGAGGTGGAATC
		R	GCGACACGTCCCATATCAGT
	Substrate-binding protein (Ga0064049_111418)	F	TGCCGACCATTTCACCAAGT
		R	TTGCTCCATGCCTTGTCGAT
	β-Galactosidase (Ga0064049_104415)	F	CGACTACGAGTCCGAATGGG
		R	GCTCGGCAATACGACCATCT
B. pseudocatenulatum SC585 gene expression	β-Galactosidase (Ga0064049_10859)	F	GATCGAACTGTTGAACGCCG
		R	CGTCAAGCAGCGTAGCAATC
	β-Galactosidase (Ga0064049_111411)	F	CGAATACACCGCCGATACCA
		R	TGCGATCCTGGTACGTTTCC
	β-Galactosidase (Ga0064049_11171)	F	CACCAAACTGTTCCGCCAAG
		R	ATCGCCGTATCGGACTGTTC
B. pseudocatenulatum MP80 protein cloning	α-Fucosidase GH29 (Ga0224696_111927	F	CACCATGAGCAATCCAACAAAT
		R	TATCCGCACCACAGCCG
	α-Fucosidase GH95 (Ga0224696_111926	F	CACCATGAAACTCACATTCGATG
		R	ACGCCGGATGGTTCCCT
	Substrate-binding protein (Ga0224696_111933	F	CACCATGAAGGACACTAAAACTGC
		R	GTCGGCGTCGGTGGT
B. pseudocatenulatum SC585 protein cloning	Substrate-binding protein	F	CACCATGAGCCAGGCTAAGAGC
		R	GTCGGCGTCAGTGGTGACCT

[a]Primers were modified from reference 49 for *B. pseudocatenulatum* DSM 20438.
[b]F, forward primer; R, reverse primer.

microplate reader, and cells were harvested at mid-log phase (OD_{600}, 0.3 to 0.7), centrifuged at 21,130 rcf, and stored in RNAlater (Ambion) at −20°C. Samples were thawed on ice, centrifuged at 4°C at 21,130 rcf for 2 min, washed with 1 ml RNase-free 1× PBS, and recentrifuged. Samples were lysed with 250 μl of 50 mg ml^{-1} lysozyme and 120 U mutanolysin at 37°C for 20 min. Lysate was centrifuged at 4°C at 9,391 rcf for 1 min,

supernatant was discarded, and pellets were processed with the RNAqueous total RNA isolation kit (Ambion) according to the kit's instructions for bacterial sample preparation and RNA extraction. RNA integrity was evaluated by agarose electrophoresis (1.2% agarose gel [wt/vol]). Subsequently, DNA was removed using the Turbo DNA-free kit (Ambion) according to the kit's instruction with an extended 1-h DNase incubation. RNA was converted to total cDNA using the high-capacity cDNA reverse transcription kit (Applied Biosystems) according to the kit's instructions and stored at −20°C until use. A 20-μl reaction mixture containing 10 μl 2× SYBR premix Ex Taq II (TIi RNase H Plus) master mix (Clontech), 0.4 μl of each primer (10 mM) (Table 5), 0.4 μl 50× ROX reference dye II, and 2 μl cDNA was run on a 7500 Fast real-time PCR system (Applied Biosystems) with a 20-s hold at 50°C, followed by 95°C for 10 min and 40 cycles of 95°C for 15 s and 60°C for 1 min. The threshold cycle ($\Delta\Delta CT$ method) was calculated and used to determine fold change in expression.

RNA-Seq screen of *B. pseudocatenulatum* MP80 transcriptome. For transcriptome screening, *B. pseudocatenulatum* MP80 was grown on basal MRS media supplemented with 1% (wt/vol) lactose, 2′-FL, or LNFP-1 in four biological replicates to understand differential expression due to various growth substrates. Cells were grown to mid-log phase with an A_{600} of 0.6 to 0.7 and stored in RNAprotect (Qiagen Inc., Valencia, CA). Cells were lysed with 250 μl (50 g/liter) lysozyme (Sigma-Aldrich, St. Louis, MO) and 120 units of mutanolysin (Sigma-Aldrich, St. Louis, MO). RNA was extracted with the RNeasy minikit (Qiagen Inc., Valencia, CA) and DNase treated twice. rRNA was depleted with the RiboMinus transcriptome isolation kit, bacteria (Thermo Fisher, Waltham, MA), while the integrity of RNA was assayed using the 2100 Bioanalyzer (Agilent Technologies, Santa Clara, CA). Barcode-indexed transcriptome-sequencing (RNA-Seq) libraries were sequenced on a NextSeq 500 (Illumina, San Diego, CA) with paired-end 75-bp reads. Sequences were processed with CLCBio Genomics Workbench (CLC Bio, Denmark), and reads were trimmed (maximum of 2 ambiguous base pairs) and deleted if the quality scores were below 0.5. Sequences were mapped to the *B. pseudocatenulatum* MP80 genome. Reads per kilobase per million (RPKM) values were calculated, and data were $\log_2$ transformed and normalized by totals. Gene expression levels in LNFP-1 and 2′-FL were compared to lactose-grown cells, and statistically significant changes were analyzed using Baggerley's test with a false-discovery rate (FDR) *P* value of ≤0.05.

Cloning and expression of *B. pseudocatenulatum* fucosidase operon genes. The SBP (Ga0224696_111933), α-fucosidase GH29 (Ga0224696_111927), and α-fucosidase GH95 (Ga0224696_111926) from *B. pseudocatenulatum* MP80 and the SBP (Ga0064049_111418) from *B. pseudocatenulatum* SP585 were cloned using the Champion pET directional TOPO expression kits (Invitrogen) according to the kit's instructions unless noted otherwise. The SBP forward primers (listed in Table 5) start with the first nucleotide (MP80 nucleotide 88 and SC585 nucleotide 91) after the predicted signal and transmembrane domains preceded by the CACC sequence and ATG start codon. A 50-μl reaction mixture with 1× Phusion HF buffer, 200 mM dNTPs, 0.5 mM each primer, 100 to 150 ng genomic DNA, and 1 U Phusion DNA polymerase (New England Biolabs, Ipswich, MA) was used. Cycling parameters are as follows: 30 s at 98°C, followed by 30 cycles of 98°C for 10 s, 64°C for 30 s, and 72°C for 45 s, with a final extension period of 5 min at 72°C. PCR amplicons were purified with QIAquick gel extraction kit (Qiagen) or DNA clean and concentrator kit (Zymo Research, Irvine, CA). Purified PCR products were cloned into the pET101 (MP80) or pET102 (SC585) dTOPO vector, transformed into One Shot Top10 chemically competent *Escherichia coli* and plated onto LB agar containing 100 μg ml^{-1} carbenicillin. Plasmid DNA from putative transformants was isolated using the QIAprep Spin miniprep kit (Qiagen). Clones were confirmed by PCR prior to transformation into chemically competent BL21star (DE3) One Shot *E. coli* and plated on LB agar containing 100 μg ml^{-1} carbenicillin. Confirmed transformants were stored in 25% (vol/vol) glycerol at −80°C.

Inoculate 200 ml of LB broth containing 100 μg ml^{-1} carbenicillin and 1% (wt/vol) glucose with 4 ml overnight cultures of BL21star transformants and incubated at 37°C with agitation at 225 rpm. At an approximately OD_{600} of 0.6, protein expression was induced with 1 mM isopropyl-β-D-1-thiogalactopyranoside and incubated 18 to 22 h. Cells were harvested by centrifugation at 3,220 rcf for 20 min at 4°C. Cell pellets were lysed in 4 ml 50 mM NaH_2PO_4, 300 mM NaCl, and 10 mM imidazole, pH 8.0, containing 90 μl 50 mg ml^{-1} lysozyme and incubated for 30 min on ice. Solution was vortexed at maximum speed for 2 min, 45 μl DNase I solution (Roche) and 5 μl RNase A (Epicentre) were added, and it was incubated for 15 min on ice. Lysates were centrifuged at 10,000 rcf for 30 min at 4°C. Supernatants were combined with nickel-nitrilotriacetic acid (Ni-NTA) agarose (Qiagen) at a ratio of 4:1 and incubated on a tilt table for 1 h at 4°C. Lysate-agarose was washed twice with 10 ml of 50 mM NaH_2PO_4, 300 mM NaCl, and 20 mM imidazole, pH 8.0, in a 5-ml disposable gravity chromatography column (Qiagen). Proteins were eluted with 4 × 500 μl of 50 mM NaH_2PO_4, 300 mM NaCl, and 250 mM imidazole, pH 8.0. Proteins were visualized by SDS-PAGE using a 7.5% 2× TGX mini-Protean gel (Bio-Rad). Imidazole buffer was exchanged for 1× PBS using Amicon Ultra 0.5-ml centrifugal filter units with a 3-kDA cutoff (EMD Millipore). Purified proteins were stored in PBS with 25% (vol/vol) glycerol at −20°C.

***B. pseudocatenulatum* MP80 and SC585 substrate-binding, protein-binding specificity.** An approximately 8-μl reaction mixture containing 10 μM substrate-binding protein and 1 μM each HMO (Tables S4 and S5 in the supplemental material) was analyzed by a catch-and-release electrospray ionization-mass spectrometry assay using a Synapt G2S ESI quadrupole-ion mobility separation-time of flight mass spectrometry (TOF MS) (Waters) equipped with a nanoflow electrospray ionization source with minor modifications (58). Briefly, a capillary voltage of 1.0 kV and a cone voltage of 30 kV (in negative ion mode) were applied, and the source block temperature was maintained at 60°C for electrospray ionization. Ion transmission was carried out with trap voltages of 10 to 80 V and transfer voltages of 2 to 60 V. The ion mobility separation parameters were optimized for each HMO isomer set as follows: trap gas flow rate at 6 ml min^{-1}, helium cell gas flow rate at 150 to 180 ml min^{-1}, ion mobility gas flow rate at 50 to 90 ml min^{-1}, trap direct-current bias at 50 V, ion mobility wave velocity at 400 to 1,000 m s^{-1}, and ion

mobility wave height at 15 to 40 V. For ion mobility separation, N_2 at 341 Pa was used. Data acquisition and processing were carried out using MassLynx (version 4.1; Waters).

Affinities of the HMOs were ranked according to the abundances of ligands released (as ions) from the protein complexes in the CaR-ESI-MS measurements. The HMOs were assigned as "low/no binding" when signal for their released ions was not detected or was detected with a low signal-to-noise ratio (i.e., S/N $\leq$ 3). HMOs for which the S/N of the released ions was $\geq$70 were assigned as "strong binding." HMO ligands with intermediate S/N (i.e., 3 $\leq$ S/N $\leq$ 70) were assigned as "medium binding."

***B. pseudocatenulatum* MP80 α-fucosidase GH29 and GH95 HMO substrate specificity.** A 1.5-μl (2 mg ml^{-1}) sample of a reduced HMO pool was digested with 2 mg ml^{-1} of purified α-fucosidase GH29 and GH95 (described above) in 10 μl of 0.1 M NH_4 acetate buffer. Reaction mixtures were incubated at each enzyme's optimal pH, temperature, and duration (data not shown) and stored at −80°C until identification of undigested HMOs (described below).

Glycoprofiling of HMOs by nano-HPLC-ChIP-TOF mass spectrometry. Cell-free supernatants and undigested HMOs were recovered, reduced, and desalted by solid-phase extraction on graphitized carbon cartridges as previously described (8). HMOs analytes were separated on a 1200 Infinity series high-performance liquid chromatography (HPLC) unit (Agilent Technologies) and detected on a 6220 series TOF LC/MS unit (Agilent Technologies), and data were processed using the MassHunter qualitative analysis software (version B.06.01; Agilent) as previously described (7, 59, 60).

Data availability. The sequenced *B. pseudocatenulatum* genomes were annotated and deposited in the Integrated Microbial Genome Expert Review annotation platform (GOLD project ID Gs0113979). Sequenced strains are located at associated IMG/JGI analysis IDs SC585 (Ga0064049), MP80 (Ga0224696), JCM7040 (Ga0024098), JCM11661 (Ga0064497), L15 (Ga0064499), and GST210 (Ga0064498) (https://img.jgi.doe.gov/). Additional genome accessions are provided in Table S3. RNA-Seq data were deposited in the NCBI GEO repository (accession no. GSE175820).

SUPPLEMENTAL MATERIAL

Supplemental material is available online only.

SUPPLEMENTAL FILE 1, PDF file, 0.3 MB.

ACKNOWLEDGMENTS

We thank Juliana de Moura Bell, Joshua Cohen, and Daniela Barile for providing purified human milk oligosaccharides and Xi Chen for providing the LNFP1. The *B. pseudocatenulatum* strain L15 was kindly provided by Eva Vlková.

This study was funded in part by UC Davis RISE program, National Institutes of Health awards AT007079 and AT008759 (D.A.M.), and the Peter J. Shields Endowed Chair in Dairy Food Science (D.A.M.).

G.S. and D.A.M. designed the study. G.S., J.L.H., B.E.H., and D.A.M. wrote the manuscript. D.A.M. secured funding for this study. G.S. conducted all experiments except as noted. J.L.H. cloned and purified *B. pseudocatenulatum* SC585's SBP. J.L.H. and B.E.H. conducted qRT-PCR of bacteria grown on 2′-FL. B.E.H. and S.W. performed RNA-Seq analysis. C.F.M. assembled the PacBio *B. pseudocatenulatum* MP80 genome. J.A.L., B.E.H., and C.M.S. analyzed the 2′-FL metabolite profile of *B. pseudocatenulatum* MP80. N.M.J. conducted the comparative genomics analysis. E.G. and C.B.L. analyzed the glycoprofiling of pooled HMO growths. A.E., L.N., and J.S.K. analyzed the binding specificity of SBP from *B. pseudocatenulatum* MP80 and SC585. All authors read, edited, and approved submission of the manuscript for publication.

D.A.M. and C.B.L. are cofounders of Evolve Biosystems and BCD Biosciences, companies with products for addressing gut health. B.E.H. currently works for Evolve Biosystems. J.L.H. currently works for Mascoma, LLC. No companies played a role in the origination, design, execution, interpretation, or publication of this work. All other authors declare no conflicts of interest.

REFERENCES

1. Smilowitz JT, O'Sullivan A, Barile D, German JB, Lönnerdal B, Slupsky CM. 2013. The human milk metabolome reveals diverse oligosaccharide profiles. J Nutr 143:1709–1718. https://doi.org/10.3945/jn.113.178772.
2. Ninonuevo MR, Park Y, Yin H, Zhang J, Ward RE, Clowers BH, German JB, Freeman SL, Killeen K, Grimm R, Lebrilla CB. 2006. A strategy for annotating the human milk glycome. J Agric Food Chem 54:7471–7480. https://doi.org/10.1021/jf0615810.
3. De Leoz MLA, Kalanetra KM, Bokulich NA, Strum JS, Underwood MA, German JB, Mills DA, Lebrilla CB. 2015. Human milk glycomics and gut microbial genomics in infant feces show a correlation between human milk oligosaccharides and gut microbiota: a proof-of-concept study. J Proteome Res 14:491–502. https://doi.org/10.1021/pr500759e.
4. LoCascio RG, Ninonuevo MR, Freeman SL, Sela DA, Grimm R, Lebrilla CB, Mills DA, German JB. 2007. Glycoprofiling of bifidobacterial consumption of human milk oligosaccharides demonstrates strain specific, preferential consumption of small chain glycans secreted in early human lactation. J Agric Food Chem 55:8914–8919. https://doi.org/10.1021/jf0710480.

5. Garrido D, Ruiz-Moyano S, Lemay DG, Sela DA, German JB, Mills DA. 2015. Comparative transcriptomics reveals key differences in the response to milk oligosaccharides of infant gut-associated bifidobacteria. Sci Rep 5:13517. https://doi.org/10.1038/srep13517.
6. Thongaram T, Hoeflinger JL, Chow J, Miller MJ. 2017. Human milk oligosaccharide consumption by probiotic and human-associated bifidobacteria and lactobacilli. J Dairy Sci 100:7825–7833. https://doi.org/10.3168/jds.2017-12753.
7. Garrido D, Ruiz-Moyano S, Kirmiz N, Davis JC, Totten SM, Lemay DG, Ugalde JA, German JB, Lebrilla CB, Mills DA. 2016. A novel gene cluster allows preferential utilization of fucosylated milk oligosaccharides in Bifidobacterium longum subsp. longum SC596. Sci Rep 6:35045. https://doi.org/10.1038/srep35045.
8. Ruiz-Moyano S, Totten SM, Garrido DA, Smilowitz JT, German JB, Lebrilla CB, Mills DA. 2013. Variation in consumption of human milk oligosaccharides by infant gut-associated strains of Bifidobacterium breve. Appl Environ Microbiol 79:6040–6049. https://doi.org/10.1128/AEM.01843-13.
9. Bunesova V, Lacroix C, Schwab C. 2016. Fucosyllactose and L-fucose utilization of infant Bifidobacterium longum and Bifidobacterium kashiwanohense. BMC Microbiol 16:248. https://doi.org/10.1186/s12866-016-0867-4.
10. Katoh T, Ojima MN, Sakanaka M, Ashida H, Gotoh A, Katayama T. 2020. Enzymatic adaptation of Bifidobacterium bifidum to host glycans, viewed from glycoside hydrolyases and carbohydrate-binding modules. Microorganisms 8:481. https://doi.org/10.3390/microorganisms8040481.
11. Gotoh A, Katoh T, Sakanaka M, Ling Y, Yamada C, Asakuma S, Urashima T, Tomabechi Y, Katayama-Ikegami A, Kurihara S, Yamamoto K, Harata G, He F, Hirose J, Kitaoka M, Okuda S, Katayama T. 2018. Sharing of human milk oligosaccharides degradants within bifidobacterial communities in faecal cultures supplemented with Bifidobacterium bifidum. Sci Rep 8:13958. https://doi.org/10.1038/s41598-018-32080-3.
12. Turroni F, Duranti S, Milani C, Lugli GA, van Sinderen D, Ventura M. 2019. Bifidobacterium bifidum: a key member of the early human gut microbiota. Microorganisms 7:544. https://doi.org/10.3390/microorganisms7110544.
13. Marcobal A, Barboza M, Sonnenburg ED, Pudlo N, Martens EC, Desai P, Lebrilla CB, Weimer BC, Mills DA, German JB, Sonnenburg JL. 2011. Bacteroides in the infant gut consume milk oligosaccharides via mucus-utilization pathways. Cell Host Microbe 10:507–514. https://doi.org/10.1016/j.chom.2011.10.007.
14. Kostopoulos I, Elzinga J, Ottman N, Klievink JT, Blijenberg B, Aalvink S, Boeren S, Mank M, Knol J, de Vos WM, Belzer C. 2020. Akkermansia muciniphila uses human milk oligosaccharides to thrive in the early life conditions in vitro. Sci Rep 10:14330. https://doi.org/10.1038/s41598-020-71113-8.
15. Pichler MJ, Yamada C, Shuoker B, Alvarez-Silva C, Gotoh A, Leth ML, Schoof E, Katoh T, Sakanaka M, Katayama T, Jin C, Karlsson NG, Arumugam M, Fushinobu S, Abou Hachem M. 2020. Butyrate producing colonic Clostridiales metabolise human milk oligosaccharides and cross feed on mucin via conserved pathways. Nat Commun 11:3285. https://doi.org/10.1038/s41467-020-17075-x.
16. Matsuki T, Yahagi K, Mori H, Matsumoto H, Hara T, Tajima S, Ogawa E, Kodama H, Yamamoto K, Yamada T, Matsumoto S, Kurokawa K. 2016. A key genetic factor for fucosyllactose utilization affects infant gut microbiota development. Nat Commun 7:11939. https://doi.org/10.1038/ncomms11939.
17. Duar RM, Henrick BM, Casaburi G, Frese SA. 2020. Integrating the ecosystem services framework to define dysbiosis of the breastfed infant gut: the role of B. infantis and human milk oligosaccharides. Front Nutr 7:33. https://doi.org/10.3389/fnut.2020.00033.
18. Sela DA, Chapman J, Adeuya A, Kim JH, Chen F, Whitehead TR, Lapidus A, Rokhsar DS, Lebrilla CB, German JB, Price NP, Richardson PM, Mills DA. 2008. The genome sequence of Bifidobacterium longum subsp. infantis reveals adaptations for milk utilization within the infant microbiome. Proc Natl Acad Sci U S A 105:18964–18969. https://doi.org/10.1073/pnas.0809584105.
19. James K, Motherway MO, Bottacini F, van Sinderen D. 2016. Bifidobacterium breve UCC2003 metabolises the human milk oligosaccharides lacto-N-tetraose and lacto-N-neo-tetraose through overlapping, yet distinct pathways. Sci Rep 6:38560. https://doi.org/10.1038/srep38560.
20. Wada J, Ando T, Kiyohara M, Ashida H, Kitaoka M, Yamaguchi M, Kumagai H, Katayama T, Yamamoto K. 2008. Bifidobacterium bifidum lacto-N-biosidase, a critical enzyme for the degradation of human milk oligosaccharides with a type 1 structure. Appl Environ Microbiol 74:3996–4004. https://doi.org/10.1128/AEM.00149-08.
21. Ashida H, Miyake A, Kiyohara M, Wada J, Yoshida E, Kumagai H, Katayama T, Yamamoto K. 2009. Two distinct alpha-L-fucosidases from Bifidobacterium bifidum are essential for the utilization of fucosylated milk oligosaccharides and glycoconjugates. Glycobiology 19:1010–1017. https://doi.org/10.1093/glycob/cwp082.
22. Katayama T, Sakuma A, Kimura T, Makimura Y, Hiratake J, Sakata K, Yamanoi T, Kumagai H, Yamamoto K. 2004. Molecular cloning and characterization of Bifidobacterium bifidum 1,2-alpha-L-fucosidase (AfcA), a novel inverting glycosidase (glycoside hydrolase family 95). J Bacteriol 186:4885–4893. https://doi.org/10.1128/JB.186.15.4885-4893.2004.
23. Shuhaimi M, Ali AM, Saleh NM, Yazid AM. 2002. Classification of Bifidobacterium isolates from infant faeces using PCR-based and 16S rDNA partial sequences analysis methods. Bioscience Microflora 21:155–161. https://doi.org/10.12938/bifidus1996.21.155.
24. Turroni F, Peano C, Pass DA, Foroni E, Severgnini M, Claesson MJ, Kerr C, Hourihane J, Murray D, Fuligni F, Gueimonde M, Margolles A, De Bellis G, O'Toole PW, van Sinderen D, Marchesi JR, Ventura M. 2012. Diversity of bifidobacteria within the infant gut microbiota. PLoS One 7:e36957. https://doi.org/10.1371/journal.pone.0036957.
25. Simeoni U, Berger B, Junick J, Blaut M, Pecquet S, Rezzonico E, Grathwohl D, Sprenger N, Brüssow H, Szajewska H, Bartoli JM, Brevaut-Malaty V, Borszewska-Kornacka M, Feleszko W, François P, Gire C, Leclaire M, Maurin JM, Schmidt S, Skórka A, Squizzaro C, Verdot JJ, Study Team. 2016. Gut microbiota analysis reveals a marked shift to bifidobacteria by a starter infant formula containing a synbiotic of bovine milk-derived oligosaccharides and Bifidobacterium animalis subsp. lactis CNCM I-3446. Environ Microbiol 18:2185–2195. https://doi.org/10.1111/1462-2920.13144.
26. Yassour M, Vatanen T, Siljander H, Hämäläinen A-M, Härkönen T, Ryhänen SJ, Franzosa EA, Vlamakis H, Huttenhower C, Gevers D, Lander ES, Knip M, Xavier RJ, DIABIMMUNE Study Group. 2016. Natural history of the infant gut microbiome and impact of antibiotic treatment on bacterial strain diversity and stability. Sci Transl Med 8:343ra81. https://doi.org/10.1126/scitranslmed.aad0917.
27. Lawson MAE, O'Neill IJ, Kujawska M, Gowrinadh Javvadi S, Wijeyesekera A, Flegg Z, Chalklen L, Hall LJ. 2020. Breast milk-derived human milk oligosaccharides promote Bifidobacterium interactions within a single ecosystem. ISME J 14:635–648. https://doi.org/10.1038/s41396-019-0553-2.
28. Turroni F, Foroni E, Pizzetti P, Giubellini V, Ribbera A, Merusi P, Cagnasso P, Bizzarri B, de'Angelis GL, Shanahan F, van Sinderen D, Ventura M. 2009. Exploring the diversity of the bifidobacterial population in the human intestinal tract. Appl Environ Microbiol 75:1534–1545. https://doi.org/10.1128/AEM.02216-08.
29. Junick J, Blaut M. 2012. Quantification of human fecal Bifidobacterium species by use of quantitative real-time PCR analysis targeting the groEL gene. Appl Environ Microbiol 78:2613–2622. https://doi.org/10.1128/AEM.07749-11.
30. Milani C, Mangifesta M, Mancabelli L, Lugli GA, James K, Duranti S, Turroni F, Ferrario C, Ossiprandi MC, van Sinderen D, Ventura M. 2017. Unveiling bifidobacterial biogeography across the mammalian branch of the tree of life. ISME J 11:2834–2847. https://doi.org/10.1038/ismej.2017.138.
31. Yatsunenko T, Rey FE, Manary MJ, Trehan I, Dominguez-Bello MG, Contreras M, Magris M, Hidalgo G, Baldassano RN, Anokhin AP, Heath AC, Warner B, Reeder J, Kuczynski J, Caporaso JG, Lozupone CA, Lauber C, Clemente JC, Knights D, Knight R, Gordon JI. 2012. Human gut microbiome viewed across age and geography. Nature 486:222–227. https://doi.org/10.1038/nature11053.
32. Odamaki T, Kato K, Sugahara H, Hashikura N, Takahashi S, Xiao J-Z, Abe F, Osawa R. 2016. Age-related changes in gut microbiota composition from newborn to centenarian: a cross-sectional study. BMC Microbiol 16:90. https://doi.org/10.1186/s12866-016-0708-5.
33. Lewis ZT, Totten SM, Smilowitz JT, Popovic M, Parker E, Lemay DG, Van Tassell ML, Miller MJ, Jin Y-S, German JB, Lebrilla CB, Mills DA. 2015. Maternal fucosyltransferase 2 status affects the gut bifidobacterial communities of breastfed infants. Microbiome 3:13. https://doi.org/10.1186/s40168-015-0071-z.
34. Bunešová V, Vlková E, Killer J, Rada V, Ročková Š. 2012. Identification of Bifidobacterium strains from faeces of lambs. Small Ruminant Res 105:355–360. https://doi.org/10.1016/j.smallrumres.2011.12.004.
35. Smilowitz JT, Lemay DG, Kalanetra KM, Chin EL, Zivkovic AM, Breck MA, German JB, Mills DA, Slupsky C, Barile D. 2017. Tolerability and safety of the intake of bovine milk oligosaccharides extracted from cheese whey in healthy human adults. J Nutr Sci 6:e6. https://doi.org/10.1017/jns.2017.2.
36. Sela DA, Garrido D, Lerno L, Wu S, Tan K, Eom H-J, Joachimiak A, Lebrilla CB, Mills DA. 2012. Bifidobacterium longum subsp. infantis ATCC 15697 α-fucosidases are active on fucosylated human milk oligosaccharides. Appl Environ Microbiol 78:795–803. https://doi.org/10.1128/AEM.06762-11.

37. Nishimoto M, Kitaoka M. 2007. Identification of N-acetylhexosamine 1-kinase in the complete lacto-N-biose I/galacto-N-biose metabolic pathway in Bifidobacterium longum. Appl Environ Microbiol 73:6444–6449. https://doi.org/10.1128/AEM.01425-07.
38. El-Hawiet A, Chen Y, Shams-Ud-Doha K, Kitova EN, Kitov PI, Bode L, Hage N, Falcone FH, Klassen JS. 2018. Screening natural libraries of human milk oligosaccharides against lectins using CaR-ESI-MS. Analyst 143:536–548. https://doi.org/10.1039/c7an01397c.
39. El-Hawiet A, Chen Y, Shams-Ud-Doha K, Kitova EN, St-Pierre Y, Klassen JS. 2017. High-throughput label- and immobilization-free screening of human milk oligosaccharides against lectins. Anal Chem 89:8713–8722. https://doi.org/10.1021/acs.analchem.7b00542.
40. Katayama T. 2016. Host-derived glycans serve as selected nutrients for the gut microbe: human milk oligosaccharides and bifidobacteria. Biosci Biotechnol Biochem 80:621–632. https://doi.org/10.1080/09168451.2015.1132153.
41. Turroni F, Milani C, Duranti S, Mahony J, van Sinderen D, Ventura M. 2018. Glycan utilization and cross-feeding activities by Bifidobacteria. Trends Microbiol 26:339–350. https://doi.org/10.1016/j.tim.2017.10.001.
42. Thomson P, Medina DA, Garrido D. 2018. Human milk oligosaccharides and infant gut bifidobacteria: molecular strategies for their utilization. Food Microbiol 75:37–46. https://doi.org/10.1016/j.fm.2017.09.001.
43. LoCascio RG, Desai P, Sela DA, Weimer B, Mills DA. 2010. Broad conservation of milk utilization genes in Bifidobacterium longum subsp. infantis as revealed by comparative genomic hybridization. Appl Environ Microbiol 76:7373–7381. https://doi.org/10.1128/AEM.00675-10.
44. Asakuma S, Hatakeyama E, Urashima T, Yoshida E, Katayama T, Yamamoto K, Kumagai H, Ashida H, Hirose J, Kitaoka M. 2011. Physiology of consumption of human milk oligosaccharides by infant gut-associated bifidobacteria. J Biol Chem 286:34583–34592. https://doi.org/10.1074/jbc.M111.248138.
45. Kwak M-J, Kwon S-K, Yoon J-K, Song JY, Seo J-G, Chung MJ, Kim JF. 2016. Evolutionary architecture of the infant-adapted group of Bifidobacterium species associated with the probiotic function. Syst Appl Microbiol 39:429–439. https://doi.org/10.1016/j.syapm.2016.07.004.
46. Sela DA. 2011. Bifidobacterial utilization of human milk oligosaccharides. Int J Food Microbiol 149:58–64. https://doi.org/10.1016/j.ijfoodmicro.2011.01.025.
47. Garrido D, Kim JH, German JB, Raybould HE, Mills DA. 2011. Oligosaccharide binding proteins from Bifidobacterium longum subsp. infantis reveal a preference for host glycans. PLoS One 6:e17315. https://doi.org/10.1371/journal.pone.0017315.
48. Sakanaka M, Hansen ME, Gotoh A, Katoh T, Yoshida K, Odamaki T, Yachi H, Sugiyama Y, Kurihara S, Hirose J, Urashima T, Xiao J-Z, Kitaoka M, Fukiya S, Yokota A, Lo Leggio L, Abou Hachem M, Katayama T. 2019. Evolutionary adaptation in fucosyllactose uptake systems supports bifidobacteria-infant symbiosis. Sci Adv 5:eaaw7696. https://doi.org/10.1126/sciadv.aaw7696.
49. Delétoile A, Passet V, Aires J, Chambaud I, Butel M-J, Smokvina T, Brisse S. 2010. Species delineation and clonal diversity in four Bifidobacterium species as revealed by multilocus sequencing. Res Microbiol 161:82–90. https://doi.org/10.1016/j.resmic.2009.12.006.
50. Gnoth MJ, Kunz C, Kinne-Saffran E, Rudloff S. 2000. Human milk oligosaccharides are minimally digested in vitro. J Nutr 130:3014–3020. https://doi.org/10.1093/jn/130.12.3014.
51. Zhao C, Wu Y, Yu H, Shah IM, Li Y, Zeng J, Liu B, Mills DA, Chen X. 2016. The one-pot multienzyme (OPME) synthesis of human blood group H antigens and a human milk oligosaccharide (HMOS) with highly active Thermosynechococcus elongates α1-2-fucosyltransferase. Chem Commun (Camb) 52:3899–3902. https://doi.org/10.1039/c5cc10646j.
52. He X, Mishchuk DO, Shah J, Weimer BC, Slupsky CM. 2013. Cross-talk between E. coli strains and a human colorectal adenocarcinoma-derived cell line. Sci Rep 3:3416. https://doi.org/10.1038/srep03416.
53. Koren S, Walenz BP, Berlin K, Miller JR, Bergman NH, Phillippy AM. 2017. Canu: scalable and accurate long-read assembly via adaptive k-mer weighting and repeat separation. Genome Res 27:722–736. https://doi.org/10.1101/gr.215087.116.
54. Melnyk RA, Hossain SS, Haney CH. 2019. Convergent gain and loss of genomic islands drive lifestyle changes in plant-associated Pseudomonas. ISME J 13:1575–1588. https://doi.org/10.1038/s41396-019-0372-5.
55. Buchfink B, Xie C, Huson DH. 2015. Fast and sensitive protein alignment using DIAMOND. Nat Methods 12:59–60. https://doi.org/10.1038/nmeth.3176.
56. Enright AJ, Van Dongen S, Ouzounis CA. 2002. An efficient algorithm for large-scale detection of protein families. Nucleic Acids Res 30:1575–1584. https://doi.org/10.1093/nar/30.7.1575.
57. Edgar RC. 2004. MUSCLE: multiple sequence alignment with high accuracy and high throughput. Nucleic Acids Res 32:1792–1797. https://doi.org/10.1093/nar/gkh340.
58. El-Hawiet A, Shoemaker GK, Daneshfar R, Kitova EN, Klassen JS. 2012. Applications of a catch and release electrospray ionization mass spectrometry assay for carbohydrate library screening. Anal Chem 84:50–58. https://doi.org/10.1021/ac202760e.
59. Wu S, Tao N, German JB, Grimm R, Lebrilla CB. 2010. Development of an annotated library of neutral human milk oligosaccharides. J Proteome Res 9:4138–4151. https://doi.org/10.1021/pr100362f.
60. Wu S, Grimm R, German JB, Lebrilla CB. 2011. Annotation and structural analysis of sialylated human milk oligosaccharides. J Proteome Res 10:856–868. https://doi.org/10.1021/pr101006u.